

Spatial analysis of complete point location data

Introduction

In this chapter, we introduce methods for the analysis of completely censused ‘population’ data. Such data can be in one of two formats, a map of individual locations or a map of sample units with area, for each of which we have a summary of population information. The second type of data will be discussed in Chapter 5, and this chapter concentrates on data of mapped point events, which we introduced in Chapter 3 in the context of graph theory and spatial graphs. The map of the locations of all ‘events’, such as individual organisms of a particular species in a study area, may have accompanying information about each event, such as tree height or condition, or may be without such additional information (see Figure 1.3a). We are considering a complete census for the entire extent of the study area, not just a sample, and in most ecological examples the map is in two dimensions, with x - y coordinates to give the positions, but we can also consider one- or three-dimensional maps, with only x or with x - y - z coordinates. We will discuss ways of treating data in both space and time, for example, with coordinates x - y - t , in Chapter 11. The methods for analysing purely spatial point event data can begin with determining the neighbours of each event and then calculating statistical measures based on the distances to those neighbours. An alternative is to have methods based on counting the events in circles of a given range of sizes, or in spatial templates of some other shape. When there is only one category of event, as in studying the spatial structure of a single-species population of mature trees, the analysis is univariate. When two kinds of events are of interest,

for example mature trees and the seedlings of a species, the analysis is bivariate. Multivariate analysis applies when there are several categories of events, as in a study of a multispecies forest community. If the events have a quantitative variable associated with them (such as stem diameter), rather than categorical (e.g. the species to which they belong), versions of what is referred to as ‘marked process’ analysis can be used. A detailed and recent treatment of point pattern methods is available in Illian *et al.* (2008) which provides more mathematical background.

All the methods described in this chapter, and the next, are unified by the concept of analysing the data using a window function or template, with which the data are selected or compared, or used as the basis for calculations of expected outcomes if a null hypothesis is true (Dale *et al.* 2002). At the end of Chapter 5 we provide a summary (Table 5.1) that illustrates this interpretation of the material covered in both chapters. In addition, there is a close relationship of all these methods with the developments of spatial graph theory, some of which we discussed in Chapter 3; we will also provide an explicit summary of those connections in Chapter 5 (see Box 5.1).

4.1 Mapped point data in two dimensions

4.1.0 Introduction: three pattern types

The first set of methods are those used to analyse maps of the positions, usually in the form of x - y coordinates, for all points or point events of a particular type, such as spruce tree stems, in a study plot. In many of these

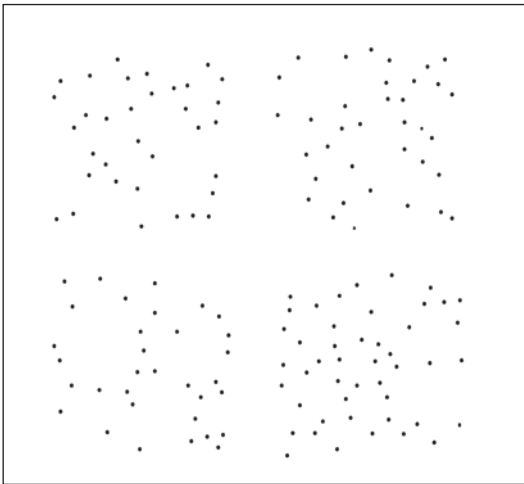


Figure 4.1 Artificial point pattern data where events only occur in the centres of the four quadrants. The events are overdispersed at small scales but underdispersed (clumped) at large scales.

methods, a test statistic is calculated from the data and then compared to the expected value of the statistic under the null hypothesis of complete spatial randomness (CSR). Many explanations of point pattern analysis offer a simple trichotomy: complete spatial randomness as a reference pattern, with clumped events or underdispersion as one alternative, and regular pattern or overdispersion as the other possibility. This trichotomy is too simple, because the appearance and interpretation of pattern can change with the scale of study; for example, if the events occur as clumps, and only one clump is examined, the events appear to be overdispersed (see Figure 4.1). To be most useful, the analysis of spatial point patterns must go beyond dividing them into the three categories and more sophisticated methods of analysis will address the issue of determining characteristics at different spatial scales, as we will illustrate below.

4.1.1 Distance to neighbours methods

Given a complete census of point events in two dimensions, one basic approach would be to measure directly, or to calculate from a map, the distances between

neighbouring events and then to determine whether the average distance is greater than or less than that expected from CSR. If the average distance is significantly less than expected, the conclusion would be that the events are clumped; if greater, that they are overdispersed.

There are, however, many different ways of defining which events are the neighbours of any particular event (see Section 3.1.1). A simple definition is to determine each event's nearest neighbour. In some cases, pairs of events will be each other's nearest neighbour, but not always.

Given a map of the positions of all events in a study area, we can choose to use only a sample of them, or we can choose to use them all. Although our focus is on complete census data, we will begin by considering a sample of events first. In using distances to study spatial pattern, it is often more convenient to use the square of the measured distances for calculating a test statistic. For example, let W_{i1} be the distance between any event i and its first nearest neighbour, and let λ be the density of events per unit area; then for a sample of the population of events, the test statistic Q , with

$$Q = \pi\lambda \sum_i^n W_{i1}^2 / n, \quad (4.1)$$

can be compared to the Normal distribution with a mean of 1 and a variance of $1/n$, often designated $N(1, 1/n)$ (Pielou 1959). This is just one of a very large number of statistics that have been proposed to study spatial point pattern, some of which compare the average distance of an event to the nearest neighbour event with the distance from a randomly placed point to its nearest event, X_{i1} . Upton & Fingleton (1985) provided a summary chart of these in their table 1.10. More sophisticated measures look at the distances not just to the first nearest neighbour but to the first nearest, the second nearest, and so on, such as W_{i3} or X_{i4} , which record the distance from event i to its third nearest neighbour and from the i th randomly placed point to the fourth nearest event. Liu (2001) provided a comparison of methods using the first to fifth nearest neighbours ($j = 1, 2, 3, 4, 5$). While different statistics have different strengths and weaknesses, his finding is

to recommend the modification of Pollard's (1971) statistic. It is

$$p(j) = 12j^2 n \left[n \ln \left(\sum_{i=1}^n X_{ij}^2 / n \right) - \sum_{i=1}^n \ln(X_{ij}^2) \right] / [(6jn + n + 1)(n - 1)]. \quad (4.2)$$

Here $p(j)$ takes the value 1 for CSR; values less than one indicate overdispersion and values greater than one indicate aggregation. The significance of departures from unity is tested by comparing $(n - 1)p(j)$ to the χ^2 distribution with $n - 1$ degrees of freedom.

For example, Figure 4.1 shows artificial data in which the events occur only in the centres of the four quadrants of the study area. This pattern was evaluated using 80 randomly placed points and Pollard's index. In this case, $p(1)$ is 1.11, which suggests clumping but is not significant, but $p(2)$ is 1.31 and $p(3)$ is 1.29, both of which are significant either by comparison with the χ^2 distribution with 79 degrees of freedom or by a Monte Carlo test with 1000 realizations of CSR. In fact, Liu (2001) suggested that $p(3)$, $p(4)$, and $p(5)$ are to be preferred.

In using all the mapped events, rather than just a sample of them, it is tempting to proceed with any one of the many methods available for sampled events. That would be wrong, of course, because if we use all of the events, the sources of information we are using are no longer independent. Using the terminology of spatial graphs introduced in Chapter 3, the nearest neighbour methods that use all mapped events are essentially using the entirety of the graph with edges defined by each node's k nearest neighbours, with $k=1$, or 2, ..., 5, or more. Thus, the location of any one event may be used in the analysis many times, as the focal event, as the first nearest neighbour of another event, as the second nearest neighbour, and so on. This may also happen when we use samples of the events for analysis, rather than them all, but with less intensity.

In addition, we need to be concerned that we are now using all the events that are close to the edge of the study plot, and there should be some

consideration of edge effects (see Chapter 1). These concerns lead to a somewhat different approach to the analysis, referred to by Diggle (1979) as 'refined' nearest neighbour analysis. Given a complete census of the locations of all events, we could use just a sample of them for analysis, as described above, provided we were willing to discard the information from those not included in the sample. Under most situations, it is preferable to adjust the method of analysis so that the full census can be used, in order to take advantage of all the information available.

4.1.2 Refined nearest neighbour analysis

Refined nearest neighbour analysis is a Monte Carlo procedure because it compares a value or set of values calculated from the data, with the same values calculated from a number of realizations of CSR using the same plot size and shape, and the same number of events. Manly (1997) illustrated one such procedure using W_{ij} , the average distance between events and their j th nearest neighbours for $j = 1$ to $j = 10$, and 499 realizations of CSR. In that example, the events are pine seedlings, and only W_1 and W_2 are significantly greater than in CSR, indicating the effects of competitive inhibition at short distances.

The approach suggested by Diggle (1979) is slightly more complicated. For any given distance, v , calculate the proportion of those events that are further than w from any boundary for which the distance to their nearest neighbour is less than w . Call that proportion $G(v)$; it is an estimate of the cumulative probability distribution of the distance from any event to its nearest neighbour event. It is sensitive to local clustering or inhibition of neighbours. If the events are randomly arranged in the plot, the expected value of $G(v)$, $E(G(v))$, is:

$$E[G(v)] = 1 - e^{-\lambda\pi v^2}. \quad (4.3)$$

One possible test statistic is the largest difference between $G(v)$ and $E(G(v))$ over the range of values of w :

$$d_w = \max |E[G(v)] - G(v)|. \quad (4.4a)$$

The observed test statistic is then compared with the values found in a 1000 or more random configurations of n events in an area the same as that of the study.

A test based on the distance between random points and their nearest neighbour event, call it u , rather than on v , can be calculated in almost exactly the same way, d_u :

$$d_u = \max |E[F(u)] - F(u)|, \quad (4.4b)$$

where F is defined for u as G was for v . $F(u)$ is an estimate of the cumulative probability distribution of the distance from a randomly chosen point to the nearest event. Because it is sensitive to gaps in the pattern of events, it is sometimes referred to as the 'empty space' function. Further insight into the spatial pattern of the events can be gained by plotting $G(v) - E(G(v))$ or $F(u) - E(F(u))$ over the range of values of w or u (see Upton & Fingleton 1985). Diggle (1979) also suggested the use of a test statistic based on the differences between the two kinds of distance functions, event–event versus point–event:

$$S_d = \sum_{i=1}^j [F(z_i) - G(z_i)], \quad (4.5)$$

where z_i represents a series of distances.

Our own experience suggests that a better choice of statistic is:

$$S_a = \sum_{i=1}^j |F(z_i) - G(z_i)|, \quad (4.6)$$

where z_i represents a series of distances.

The reason for this suggestion is that it is possible for the positive and negative differences to cancel each other out, even if they exceed, in places, the randomization envelopes (Figure 4.2). The example of living lodgepole pine (*Pinus contorta* Loudon) stems at the Fort Assiniboine site is given in Figure 4.3, with the difference between F and G plotted as a function of z . It illustrates the large-scale clumping of these stems, but does not detect significant overdispersion at smaller scales.

Again, the evaluation of either choice of test statistic would be based on comparison with the range of values found in a large number of CSR realizations. One advantage of this approach is that the test can be modified to use any distribution for comparison, not just the Poisson that is associated with CSR as the null hypothesis. Illian *et al.* (2008) provided some

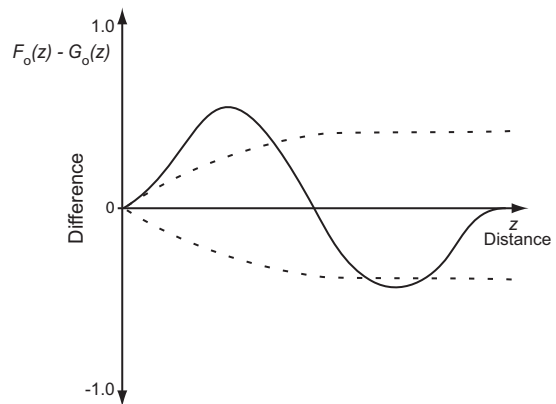


Figure 4.2 Artificial example of Diggle's difference statistic where positive and negative differences may cancel each other out.

guidance on this approach based on different models, which clearly has the advantage of determining more information on the characteristics of the observed point pattern and the point process that may underlie it.

4.1.3 Second-order point pattern analysis

The next set of methods for the mapped positions of events in the plane, such as the stems of trees, assumes a complete census of the objects of interest in the area. One of the most commonly used methods is called Ripley's K (Ripley 1976). The approach is based on the concept that, if λ is the density of events per unit area, the expected number of points in a circle radius t centred on a randomly chosen point is $\lambda K(t)$, where $K(t)$ is some function of t that depends on the pattern of the points. For example, if the points are overdispersed, $K(t)$ will be close to 0 for small radii and increase for larger distances.

The calculation of the statistic for a given radius, t , is based on counting all pairs of points separated by distance less than t . The statistic $\hat{K}(t)$ is an estimate of $K(t)$:

$$\hat{K}(t) = A \sum_{\substack{i=1 \\ i \neq j}}^n \sum_{\substack{j=1 \\ j \neq i}}^n w_{ij} I_t(i, j) / n^2, \quad (4.7a)$$

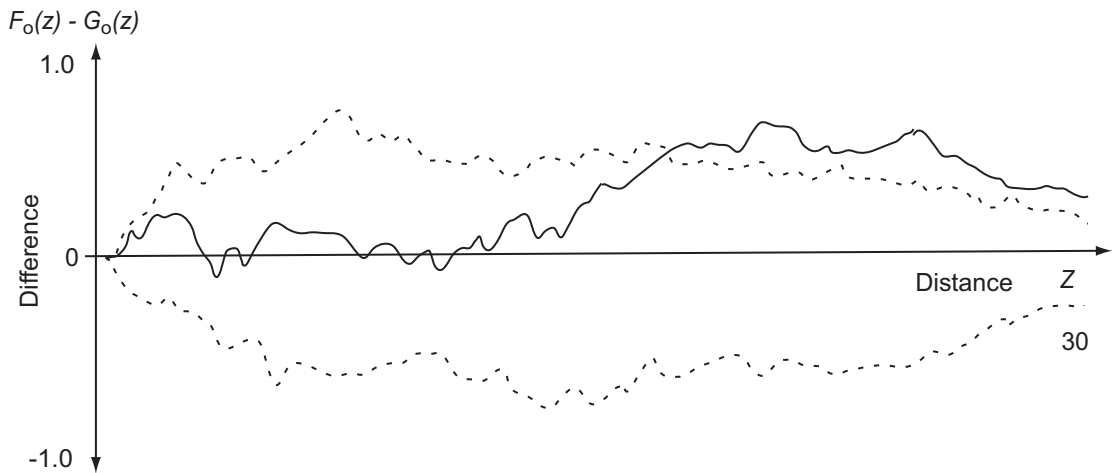


Figure 4.3 Refined neighbour analysis on living lodgepole pine trees at Fort Assiniboine (data in Figure 4.5a), where $F_o(z) - G_o(z)$ is the difference between event-event and point-event functions for a suitable chosen distance z .

where A is the area of the plot, with d_{ij} being the distance between points i and j , $I_t(i, j)$ an indicator function, taking the value 1 if $d_{ij} \leq t$ and 0 otherwise, and w_{ij} is a weight that corrects for edge effects. If the circle centred on i with radius d_{ij} is completely within the study plot, $w_{ij} = 1$; otherwise it is the reciprocal of the proportion of that circle's circumference within the plot (Diggle 1983). A number of authors have provided explicit formulae for edge corrections based on geometric arguments (Haase 1995; Goreaud & Pélissier 1999). These can be complicated and an alternative is to use a 'quick and dirty' numerical estimation by dividing the circumference into many sectors, say 120, and counting how many of them are within the boundaries of the study area.

Our own investigations suggest that the weight w_{ij} can be replaced with a weight that depends on i and t , rather than on i and j : weight $h_i(t) = 1$ if the circle centred on i with radius t is completely within the study plot, otherwise the reciprocal of the proportion of that circle's area within the plot:

$$\hat{K}(t) = A \sum_{\substack{i=1 \\ i \neq j}}^n \sum_{\substack{j=1 \\ j \neq i}}^n h_i(t) I_t(i, j) / n^2. \quad (4.7b)$$

This approach reduces the number of calculations that need to be made: one weight for each event and each

radius, rather than one for each pair of points and each radius. Again, because of the complexities of a strictly geometric calculation, a numerical estimation can be achieved by dividing the area of the circle into a large number of radial sectors, say 600 (where we suggested 120 for the circumference), and counting the number that fall within the boundary (Figure 4.4). This approach makes it possible to deal with boundaries with irregular shapes. For further discussion of edge correction techniques see Ripley (1988), Cressie (1993), Haase (1995), Gignoux *et al.* (1999) and Illian *et al.* (2008).

If the events follow CSR, the number of points in a circle follows a Poisson distribution and the expected number of events in a circle of radius t is $\pi t^2 / A$. $\hat{K}(t)$ is compared with this expected value by subtracting the observed from the expected:

$$\hat{L}(t) = t - \sqrt{\hat{K}(t) / \pi}. \quad (4.8)$$

In some versions, the expected is subtracted from the observed (e.g. Bailey & Gatrell 1995) and in interpreting results, the reader needs to be careful to determine which version is being used! The square root in the transformation has additional advantages, such as stabilizing the variance as a function of scale (see, for

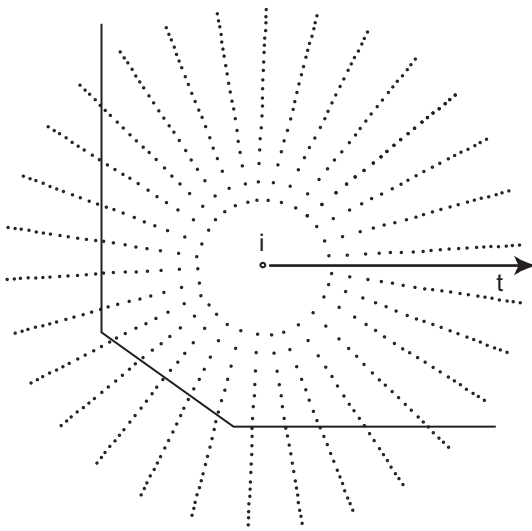


Figure 4.4 An illustration of the edge correction method for plots with irregular boundaries; the number of radial sectors within the plot is calculated.

example, Illian *et al.* 2008 for mathematical details). $\hat{L}(t)$, as given in Eq. (4.8), is plotted as a function of t , with negative values indicating clumping and positive values indicating overdispersion. (As a mnemonic, remember that under the line means underdispersed; over the line means overdispersed.) For example, Figure 4.5b shows the analysis of the data in Figure 4.5a, a map of the living lodgepole pine trees in the Fort Assiniboine example; the features of the data are clear in the analysis: overdispersion at scales less than a metre and clumping at all larger scales.

The results of the analysis can be assessed using the approximate confidence intervals for $\hat{L}(t) = 0$ provided by Ripley (1976) of $\pm 1.42(A^{1/2})/n$ for $\alpha = 5\%$ or $\pm 1.68(A^{1/2})/n$ for $\alpha = 1\%$. Using that criterion, in Figure 4.5b, the value at 0.375 m is significantly large, and values at distances greater than 2 m are significantly less than 0. In many published accounts, authors have used Monte Carlo techniques (cf. Manly 1997) to evaluate the significance of the results, thus avoiding problems of distribution theory (Andersen 1992; Haase 1995). This is the approach we recommend, and Figure 4.5b shows the 99% envelope generated from 100 realizations of CSR. As in many such situations, use of the

Monte Carlo approach makes it possible, in theory at least, to use a dispersion pattern other than CSR as the hypothesis for comparison. For example, several authors, including Reich *et al.* (1997), have used the Neyman–Scott process as a null model; it is based on completely random *clusters* of events (not random *events* as in CSR), in each of which the number of events follows a Poisson distribution. (Pielou 1977b, p.119, refers to this as a Neyman Type A or Poisson–Poisson distribution.) Kenkel (1993) found that populations of the clonal plant *Aralia nudicaulis* were well described by a Markov model with an inhibition distance of 18 cm, corresponding to the radius of the plant's shoots.

For comparison with approaches that explicitly cite the use of spatial graphs described in Chapter 3, counting all pairs of events separated by distance less than t , is the same as creating a graph with the events as the nodes and the graph's edges determined by a simple threshold distance rule that joins all pairs of nodes separated by distance no greater than t . This graph edge rule is the same as the use of a template that is a circle of radius t . There is another and different aspect to the comparison between the Ripley approach to point pattern analysis and the use of graphs in spatial analysis. Given any graph of connections between point events, we can calculate $\hat{K}(p)$, which is the average number of events (the nodes of the graph) connected to any node of the graph by a path of p edges or fewer (cf. Illian *et al.* 2008). It is therefore based on the graph theoretic distance between events, rather than the physical distance we are accustomed to in this context. These two comparisons between familiar distance-based methods and graph theoretical approaches suggest that there is much more research to be done in developing helpful variants of methods that already exist.

In Chapters 1 and 2, we made the distinction between global analysis, which evaluates the characteristics of the spatial pattern over the whole study area (perhaps with the implicit assumption of stationarity), and local analysis, which makes explicit the differences in the pattern observed among parts of the study area. The discussion of second-order statistics for point patterns has, so far, been global, but the method can be

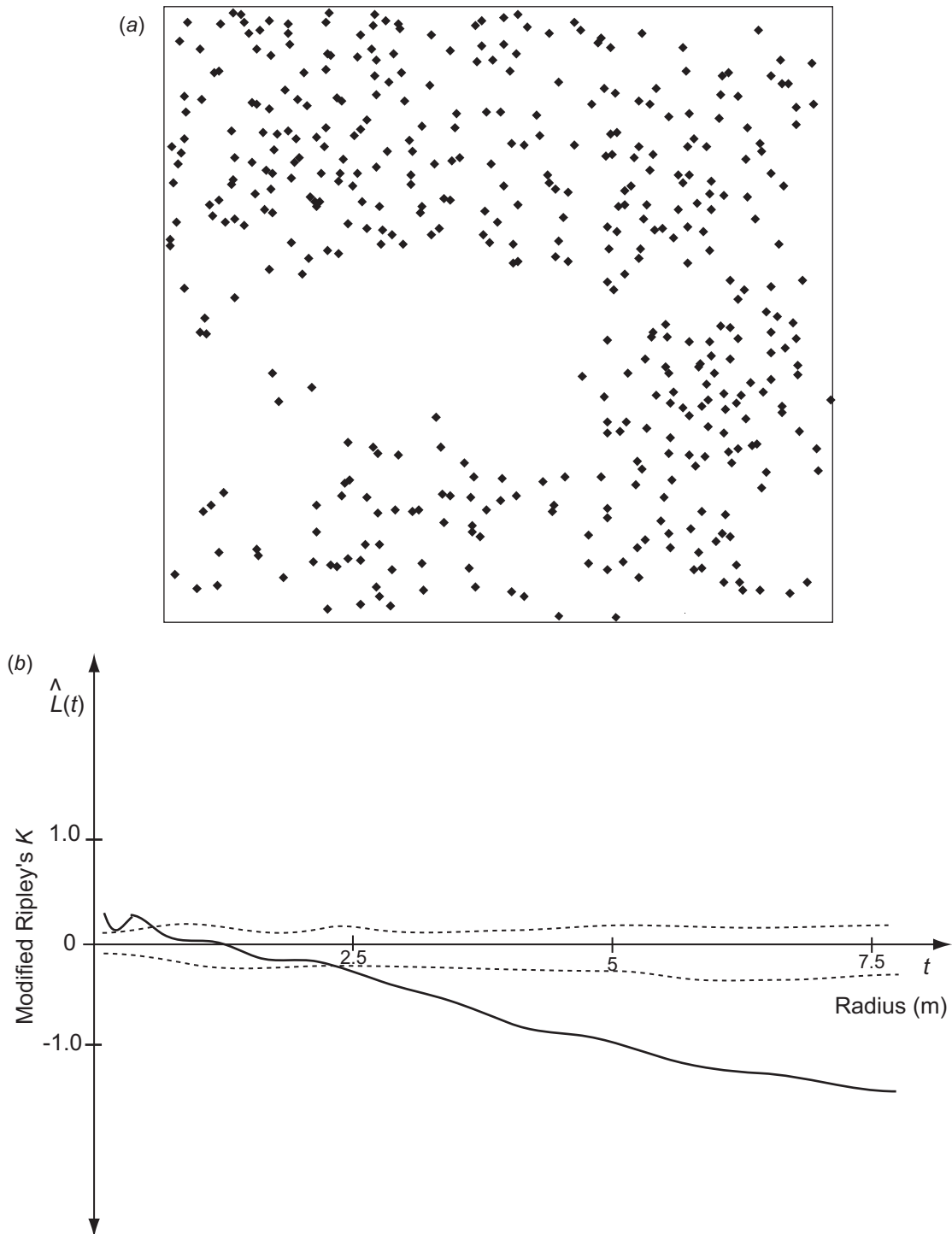
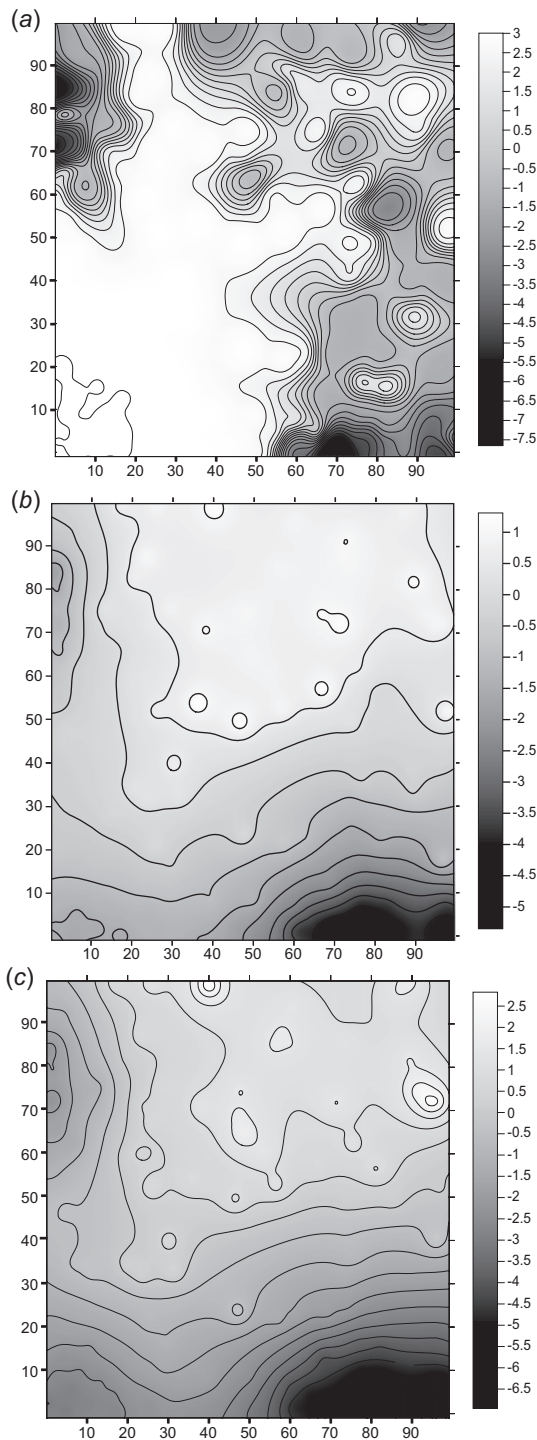


Figure 4.5 (a) Map of living lodgepole pine at Fort Assiniboine, Alberta. The plot is 50 m on each side. (b) Standardized univariate Ripley's K -function analysis of living lodgepole pine at Fort Assiniboine, Alberta, where $\hat{L}(t)$ is Ripley's standardized statistic and t is distance.



adapted to produce a spatially explicit result (cf. Getis & Franklin 1987). For each event, i , and distance, t , a score can be assigned to the position of the event that compares the observed count of events in the circle radius t centred on event i with the expected count based on the area of the circle and CSR. Contour maps of those scores can then be drawn, for particular ranges of radii, to make interpretation easy. Getis & Franklin (1987) suggested including the scores for randomly or regularly placed points that are not events, as well as those of events, so that the regions where events are sparse can be included in the analysis. This parallels, for K -function analysis, the inclusion of the 'empty space' function in refined nearest neighbour analysis described above. The authors provide examples of this technique, which give us the option of adding spatially explicit results to Ripley's K -function approach. Figure 4.6 illustrates this approach using artificial data in which the events are overdispersed in the bottom left corner (hard-core repulsion of 5 m) but clumped or random elsewhere in the 100×100 m square. Figure 4.6a–c show the L -transform scores of Ripley's K -function, Eq. (4.8) for 3 m, 10 m, and 20 m. These spatially explicit results clearly show the non-stationarity in the pattern of events, and this kind of evaluation should prove very useful in the exploration of the characteristics of some data sets in ecological studies.

In a study of the demography of a palm tree species of the humid savanna of West Africa (Ivory Coast), Barot *et al.* (1999) demonstrated the advantages of using a complementary group of methods, rather than a single one, for spatial pattern analysis. They applied Diggle's F - and G -functions (nearest neighbour and empty space functions) together with Ripley's K -function. They commented that the simultaneous use of all three functions found significant departures from CSR that would not have been evident

Figure 4.6 (a) A 'Getis' map of $\hat{L}(t)$ scores for artificial data ($100 \text{ m} \times 100 \text{ m}$) with hard-core repulsion in the lower left corner: $t = 3 \text{ m}$. (b) As (a) for $t = 10 \text{ m}$. (c) As (a) for $t = 20 \text{ m}$. Note that the ranges of values are different in the three parts of the figure.

otherwise. The situation investigated included the clumping of young seedlings around maternal trees, selective mortality restricting most juveniles to nutrient-rich patches, and subsequent self-thinning due to competition in patches of high density. Their findings confirm the suggestion that it is often a good idea to use some kind of combined analysis, using more than one method to characterize the spatial structure being investigated.

4.1.4 Bivariate data

The approaches discussed in this chapter so far can be easily modified for bivariate data, for which we want to analyse the spatial relationship of two different kinds of events, such as males or females, flowering or vegetative plants, diseased or healthy individuals, and so on. For example, Diggle's nearest neighbour function, G , can be adapted for bivariate data by examining the distance from events of Type 1 to nearest neighbour of Type 2, which gives G_{12} , separately from examining the distance from events of Type 2 to nearest neighbours of Type 1, which gives G_{21} . This separation permits the detection of asymmetric associations, which can be very useful in some circumstances, such as studying the association between mature female palm trees and seedlings (see Barot *et al.* 1999). Similarly, for bivariate data, the 'empty space' function can be divided into two parts: F_1 describing the distance from a random point to an event of Type 1 and F_2 describing the distance from a random point to an event of Type 2.

For an analysis of bivariate point event data based on Ripley's K -function, the basic question becomes this: At what scales are the two kinds of events segregated from each other, and at what scales are they aggregated? We proceed by calculating:

$$\hat{K}_{12}(t) = A \sum_{\substack{i=1 \\ i \neq j}}^{n_1} \sum_{\substack{j=1 \\ j \neq i}}^{n_2} w_{ij} I_t(i, j) / n_1 n_2 \quad (4.9)$$

and

$$\hat{K}_{21}(t) = A \sum_{\substack{i=1 \\ i \neq j}}^{n_1} \sum_{\substack{j=1 \\ j \neq i}}^{n_2} w_{ji} I_t(j, i) / n_1 n_2.$$

The two versions are both estimates of the same function and are combined as a weighted average to compare the observed and the expected:

$$\hat{L}_{12}(t) = t - \sqrt{[n_2 \hat{K}_{12}(t) + n_1 \hat{K}_{21}(t)] / \pi(n_1 + n_2)} \quad (4.10)$$

(cf. Upton & Fingleton 1985; Andersen 1992). Values greater than 0 indicate segregation and values below 0 indicate aggregation of the two different kinds of events (points) (Figures 4.7a, b). This example shows the relationship between canopy trees (mainly pine) and understorey seedlings (mainly spruce) near Grande Cache, Alberta (Dale & Powell 2001). The trees and seedlings are segregated from each other at small scales but aggregated over a range of larger scales.

A different, but closely related, approach was suggested by Diggle & Chetwynd (1991), based on Ripley's K -function, calculated separately for the two types of events:

$$\hat{K}_{11}(t) = A \sum_{\substack{i=1 \\ i \neq j}}^{n_1} \sum_{\substack{j=1 \\ j \neq i}}^{n_1} w_{ij} I_t(i, j) / n_1^2 \quad (4.11)$$

and

$$\hat{K}_{22}(t) = A \sum_{\substack{i=1 \\ i \neq j}}^{n_2} \sum_{\substack{j=1 \\ j \neq i}}^{n_2} w_{ij} I_t(i, j) / n_2^2.$$

The statistic of interest is then the difference between these two:

$$\hat{D}_{12}(t) = \hat{K}_{11}(t) - \hat{K}_{22}(t). \quad (4.12)$$

Assessment of significance is again by a Monte Carlo approach. The distances at which the statistic exceeds its envelope are the scales at which the events of the first type are clustered more than all the events combined. The properties and usefulness of this statistic require further investigation; our own informal trials suggest that the statistic might be more stable if the square roots of the K -functions were used. In addition, this statistic is probably most useful when used in combination with other methods. For example, if the statistic takes values close to zero at all scales, all that you learn is that the two types of event have similar spatial patterns, but the characteristics of those

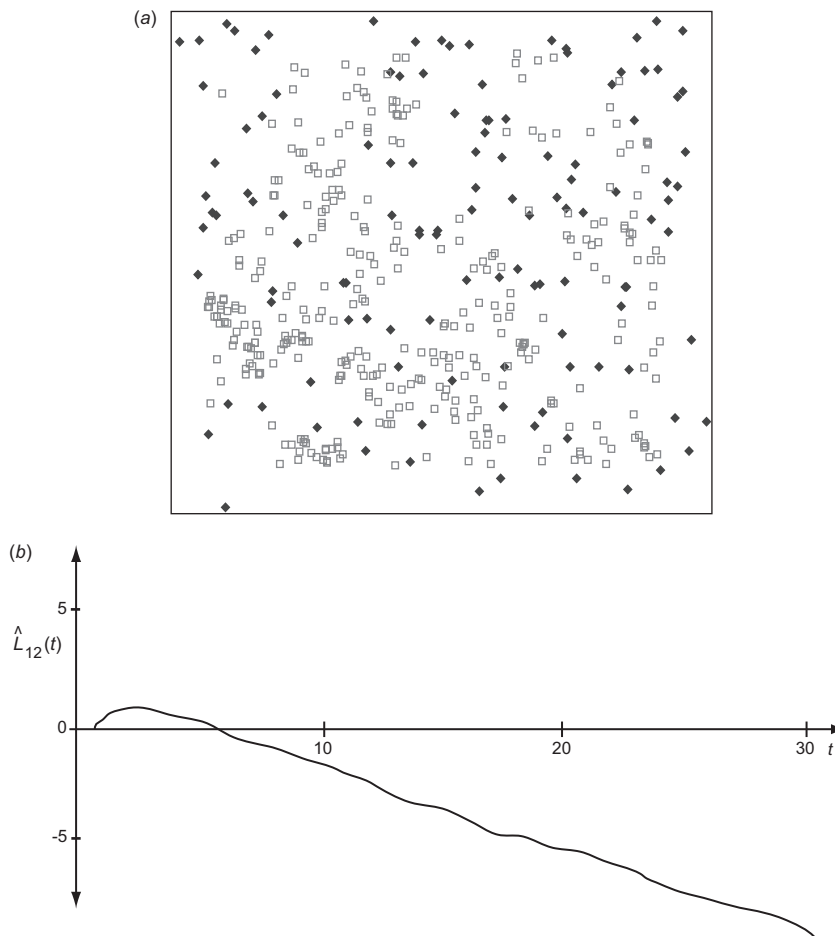


Figure 4.7 (a) Map of canopy trees (closed diamonds) and seedlings (open squares) in a 50×50 m plot near Grande Cache, Alberta. (b) Bivariate Ripley's K analysis of canopy trees and seedlings shown in (a); \hat{L} is the standardized Ripley's K and t is distance. (c) Bivariate data: re-labelling for significance testing by randomization; the events' positions are fixed but the labels are redistributed (left: original data; right: labels randomized).

patterns are not detected. The addition of one or two separate complementary analyses would make the situation clear.

As another example of the application of Ripley's bivariate K -function analysis, we can cite the work of Melles *et al.* (2009) who used the approach, in a study of the Hooded Warbler, to determine whether there was a relationship between the locations of unmated male birds and the locations of the nests. They found

that the nest sites tend to be clustered, but that clustering does not have a significant relationship with the spatial locations of the unmated males. In this example, Monte Carlo tests were used to assess the spatial aggregation of females at different spatial scales.

Bivariate patterns are amenable to significance testing by randomization. The positions of events are retained but their 'labels' (the type to which they

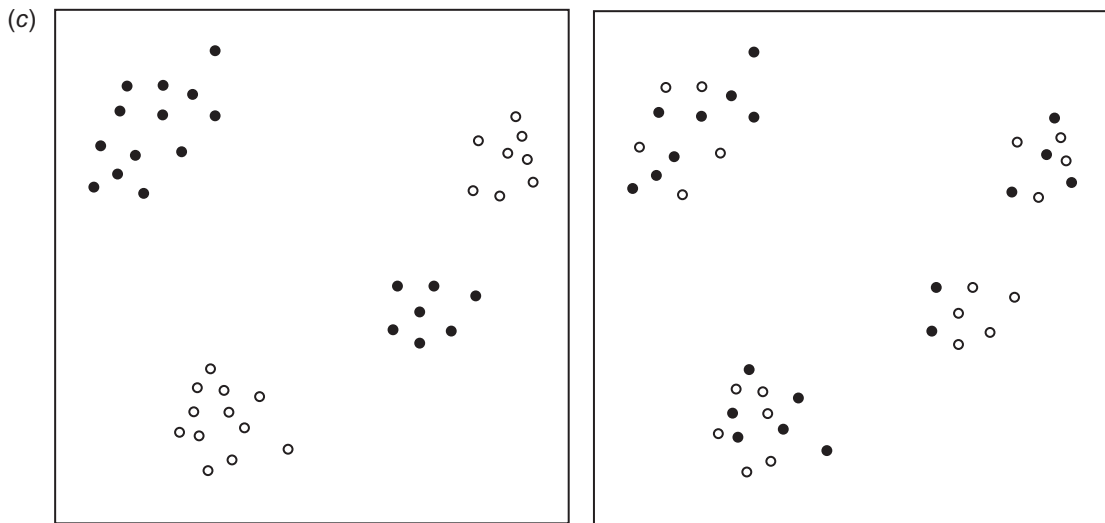


Figure 4.7 (cont.)

belong) are randomized (Figure 4.7c). This makes it possible to determine whether the events of one kind, for example, diseased organisms, are more clustered than can be explained by the overall nonrandomness of the pattern as a whole. Dale & Powell (1994) provided the example of the positions of plants of *Solidago canadensis* L., growing at the edge of a hay field, classified into two categories depending on whether the plant had obvious signs of insect attack, usually stem galls. In the *Solidago* data, based on a comparison of K_{12} with the results expected from CSR, in one quadrat (called quadrat 5 in that data set), the two kinds of plants appear aggregated over a range of scales, but a randomization of the labels shows that this is a result of overall clumping of plants of either kind (Figure 4.8a). In contrast, another quadrat (quadrat 10) from the same data set gives results for K_{12} that seem compatible with independence (values close to 0), but random re-labelling shows that the two kinds of plants are actually segregated within the overall pattern (Figure 4.8b).

This example provides one half of a contrast between two approaches to the evaluation of clusters of disease incidence: the contrast between cases in

which all individuals, diseased or not, are known, and cases where only the disease has been recorded. Whereas with our *Solidago* study, we had records of the positions of plants that were unaffected, many studies of disease in populations concentrate on analysing records of disease incidence, not including the entire 'at risk' population, whether from choice or because the information is not available. A common approach in epidemiology is to detect clusters of disease incidence (see our brief description of 'scan statistics', Section 6.6 of this book), but their interpretation may require an assessment of the background patterns as well as an understanding of the technical aspects and assumptions (see Tango 2010). It is not always possible to distinguish the clusters of disease from the overall pattern of the organisms' spatial pattern, as we were able to do in this example. We will return to the question of how clusters can be detected and evaluated.

4.1.5 Multivariate point pattern analysis data

An obvious extension of the analysis of bivariate data is to consider several types of events using

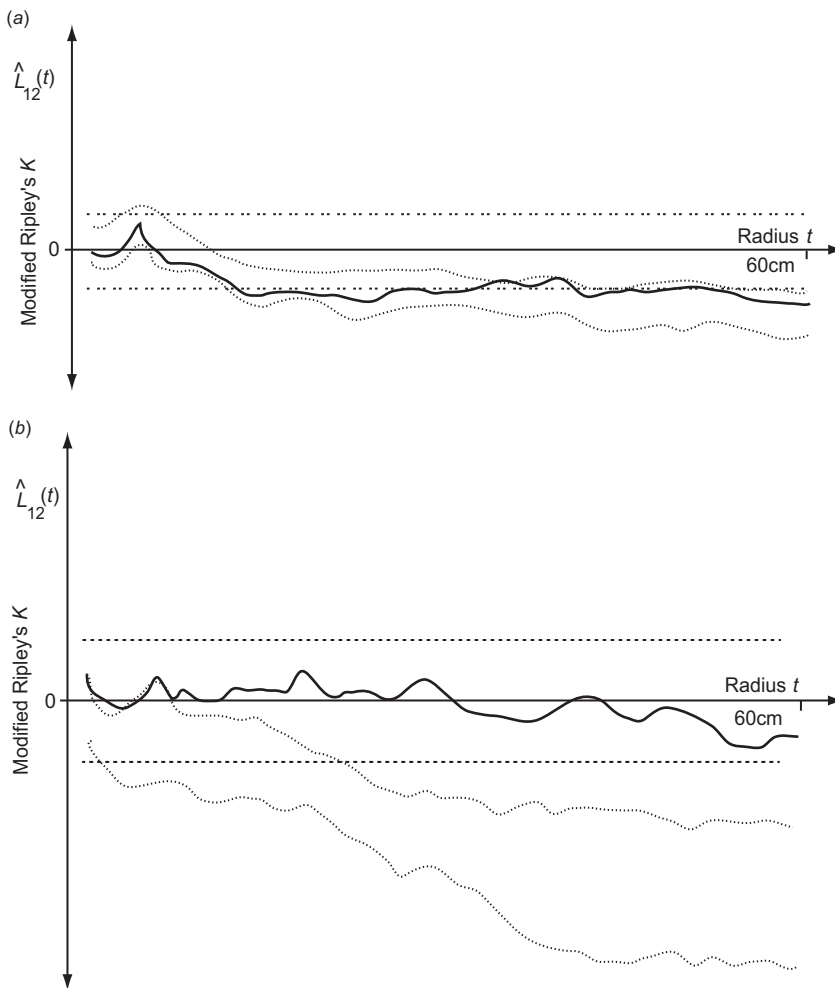


Figure 4.8 (a) Bivariate Ripley's K analysis on infected and healthy *Solidago* plants, where L_{12} is standardized Ripley's K and t is distance (quadrat 5). (b) Bivariate Ripley's K analysis on infected and healthy *Solidago* plants with randomization envelope (quadrat 10).

multivariate analysis of point patterns. Lotwick & Silberman (1982) assessed multivariate point pattern analysis and concluded that there were two basic approaches:

- (1) methods based on nearest neighbour and empty space functions (described above under 'refined nearest neighbour' methods, Section 4.1.2), and
- (2) methods based on second-order analysis (such as Ripley's K -function, Section 4.1.3).

There is a close conceptual relationship between the two approaches, which we can describe informally by comparing the basic questions asked.

- (1) Nearest neighbour methods are based on the following question: how big can a circle centred on an event (or on a random point) grow before it encounters another event?
- (2) Second-order methods are based on the following question: given a circle of a given size,

centred on an event, how many other events does it contain?

The difference is that the first is based on a maximal empty circle and the second is based on counting events in circles of a given size. We will describe methods based on nearest neighbours first before proceeding to discuss the second-order approach.

Summary statistics for quantifying several forms of dependence between events of different types in a multivariate point pattern were introduced by van Lieshout & Baddeley (1999). In the univariate context, we introduced the 'event-to-nearest-event' function, $G(t)$, and the 'point-to-nearest-event' function, $F(t)$, also called the 'empty space' function. These can be examined separately, or they can be combined to produce a univariate index of spatial interaction:

$$H(t) = \frac{1 - G(t)}{1 - F(t)}. \quad (4.13)$$

The index takes a value close to 1 under CSR, values less than 1 for clustered patterns, and values greater than 1 for overdispersed patterns.

To adapt this index for multivariate pattern, we consider having S types (e.g. species) and revise the notation for the two kinds of functions (using I and J to denote types, reserving i and j to denote individual events).

$G_{IJ}(t)$ is the distance function for events of Type I to events of Type J .

$G_{..}(t)$ is the distance function for events of any type to events of any type.

$F_J(t)$ is the empty space function from random points to events of Type J .

$F_{..}(t)$ is the empty space function from random points to events of any type.

These can then be used to define two different H -functions:

$$H_{IJ}(t) = \frac{1 - G_{IJ}(t)}{1 - F_J(t)}, \text{ for a particular pair of types } I \text{ and } J \quad (4.14a)$$

and

$$H_{..}(t) = \frac{1 - G_{..}(t)}{1 - F_{..}(t)}, \text{ for pairs of any type.} \quad (4.14b)$$

Last, with λ_I being the intensity of the I th type, and total intensity $\lambda_{..}$, an overall index can be defined as:

$$I(t) = \sum_{I=1}^S \frac{\lambda_I}{\lambda_{..}} H_{II}(t) - H_{..}(t). \quad (4.15)$$

The use of this index is illustrated in Figure 4.9. The artificial data are shown in part (a) of the figure; in Figure 4.9b, the index shows that the four species are, in general, segregated from each other, most strongly at a distance that is 20% of the length of the sample plot.

A second approach to multivariate point pattern analysis using nearest neighbours was elaborated by Dixon (2002). With S types of events, a $S \times S$ contingency table is created, with the entry in the I th row and J th column, m_{IJ} , recording the number of times that the nearest neighbour of an event of Type I was an event of Type J . This approach is very much like the analysis of neighbour contact data to detect interspecific association, as previously discussed by a number of authors including Yarranton (1966), de Jong *et al.* (1980), and Dale *et al.* (1991). In addition to being able to perform a test of the departure from expectation for the table as a whole, individual entries can be evaluated using the normal approximation:

$$Z_{IJ} = \frac{m_{IJ} - E(m_{IJ})}{\sqrt{\text{Var}(m_{IJ})}}. \quad (4.16)$$

Formulae for the calculation of the expected values and variances are given in Dixon (2002).

An example is provided in Table 4.1, using the data in Reich *et al.* (1997) from a 3×3 m study plot in short grass prairie near Fort Collins, Colorado. The dominant species were *Bouteloua gracilis* ('Bogr'), *Agropyron smithii* ('Agsm'), *Oryzopsis hymenoides* ('Orhy'), and *Stipa comata* ('Stco'), with the dicots being lumped into the category 'forbs'. The major feature of the table is that individual species had a strong tendency to be their own neighbour, as indicated by the large positive z_{II} values. This tendency was not observed for the category 'forbs'.

Dixon (2002) also provided an index of segregation of the I th type, based on the excess of within-type nearest neighbours:

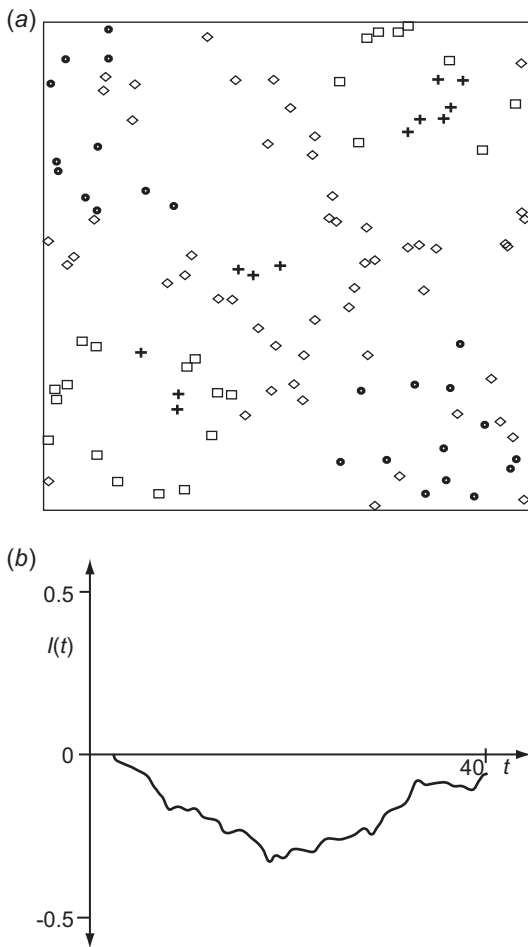


Figure 4.9 (a) Artificial multispecies point pattern data for illustration of the analysis. (b) Multivariate point pattern analysis on artificial multispecies data: $I(t)$ is the multivariate pattern index and t is distance.

$$S_I = \log \left[\frac{m_{II}/m_{I,\sim I}}{E(m_{II})/E(m_{I,\sim I})} \right] = \log \left[\frac{m_{II}/(n_I - m_{II})}{(n_I - 1)/(N - n_I)} \right]. \quad (4.17)$$

This measure looks straightforward and easy to apply and Dixon (2002) provided an example.

There are two features of Dixon's nearest neighbour method that are noteworthy in comparison with other techniques described in this section. The first

comment is that while the method uses the nearest neighbours of events, it does not use the distances to those neighbours in any of the calculations. The second comment is that because the procedure involves the development of a contingency table of the frequencies of neighbouring pair types, the method is not necessarily limited to the use of the first nearest neighbour. It could be extended to include the first and second nearest neighbours together, for example, or separate contingency tables could be set up for each of the first, second, and third nearest neighbour frequencies. In Chapter 3, we described a hierarchy of neighbour networks (also spatial graphs), and the contingency table approach could be applied to a full range of definitions of which pairs of events are neighbours.

The data used here to illustrate Dixon's method were originally used in the description of another method for multivariate point pattern analysis, developed by Reich *et al.* (1997), based on all the distances between events of the same type. In graph theoretic terms, this approach is based on the average lengths of the edges of complete graphs, the nodes of which are all the events belonging to a single type. Let the total number of events be N , but not all of them can be assigned to known taxa, as is often the case in plant ecology. We have S identified groups, G_1 to G_S , and one group for the unidentified, the 'other' category. If there are N' identified events and n_I in the I th group then:

$$C_I = n_I/N'. \quad (4.18)$$

The analysis is based on the average distance between members of a group:

$$\zeta_I = \sum_{i=1}^{N'-1} \sum_{k=j+1}^{N'} (d_{jk} | j \in G_I \& k \in G_I) / \binom{n_I}{2}. \quad (4.19)$$

Thus there are $S + 1$ complete graphs, with n_I nodes and $n_I(n_I - 1)/2$ edges to be averaged in the I th graph. The test statistic is then the weighted within-group average:

$$\delta = \sum_{I=1}^S C_I \zeta_I. \quad (4.20)$$

Table 4.1 Dixon's nearest neighbour method: short grass prairie data from Reich et al. (1997)

I^a	J^a	Obs ^b	Exp		
From:	To:	m_{IJ}	m_{IJ}	z_{IJ}	Significance
Bogr	Bogr	89	49.2	5.49	*
	Agsm	49	64.9	-2.39	*
	Orhy	28	37.9	-1.81	
	Stco	37	43.4	-1.12	
	Forbs	12	18.5	-1.63	
Agsm	Bogr	53	84.9	-3.62	*
	Agsm	169	64.9	15.58	*
	Orhy	48	49.8	-0.28	
	Stco	41	57.0	-2.44	*
	Forbs	28	24.3	0.82	
Orhy	Bogr	28	28.9	-0.15	
	Agsm	44	37.9	1.12	
	Orhy	89	49.8	6.31	*
	Stco	18	33.3	-3.01	*
	Forbs	16	14.2	0.52	
Stco	Bogr	40	38.0	0.31	
	Agsm	44	43.4	0.10	
	Orhy	15	57.0	-6.40	*
	Stco	101	33.3	13.34	*
	Forbs	19	16.2	0.78	
Forbs	Bogr	14	6.8	2.33	*
	Agsm	22	18.5	0.88	
	Orhy	21	24.3	-0.72	
	Stco	22	14.2	2.23	*
	Forbs	16	16.2	-0.06	

^a The species are Bogr = *Bouteloua gracilis*, Agsm = *Agropyron smithii*, Orhy = *Oryzopsis hymenoides* and Stco = *Stipa comata*.

^b Bold font highlights intraspecific frequencies and results.

An analytic evaluation of this statistic is possible, based on the number of possible assignments of N events to $S + 1$ groups, but a Monte Carlo test or a randomization procedure based on re-labelling the events is straightforward and easy to implement. One advantage of this approach is that different species can be examined separately using the observed values of ζ . Another advantage is that CSR is not the only null model that can be used and evaluated, and, as noted above, these authors made use of the Neyman-Scott model for comparison. A disadvantage is that if there is more than one scale of pattern in the data, the average

within-group distance may not be informative because it includes distances generated by different scales of pattern. This disadvantage is related to the difference between local and global measures of spatial pattern; a local version of this technique exists in which the average distances between events of the same type is calculated and then mapped. Reich *et al.* (1997) considered using an upper limit to the distances that is somehow related to 'cluster size'. It is not clear how effective this modification would be if there were several scales of pattern or if different species or groups of species had markedly different cluster sizes. Prior

analysis using some version of Ripley's K or other exploratory technique might be a useful preliminary step, and we will now describe the multivariate version of Ripley's K .

It is clear that, given multivariate point patterns, each type or species can be analysed separately using the univariate version of Ripley's K -function. Pairs of species can be analysed using the bivariate version too, but it is not clear what a truly multivariate analysis, based on many species at once rather than many pairs of species, would involve. The technique used will depend on the hypothesis that is of interest: for example, there is a difference between 'Do all species tend to be segregated from any other species considered individually?' and 'Do all species tend to be segregated from all other species considered together?' It is a matter of 'partitioning' the overall pattern of events into those attributable to individual types and those attributable to the relationships among types.

In their review of approaches to multivariate point pattern analysis, Lotwick & Silverman (1982) made the interesting comment that 'Not surprisingly, description and estimation of the second order structure of a multitype process requires consideration of only two of the types at a time'. This statement is not quite true, in our opinion, because while there are insights to be gained from looking at all possible intraspecific statistics of Type $K_{II}(t)$, there is also much to be learned from examining interspecific statistics of Type $K_{I \sim I}(t)$ or $K_{I \sim J}(t)$. In effect, we suggest partitioning $K_{..}(t)$, which includes all events pairs of any species combination, into $K_{XX}(t)$, which considers all conspecific pairs of events, and $K_{X \sim X}(t)$, which considers all interspecific pairs of events. $K_{XX}(t)$ can be partitioned into S possible $K_{II}(t)$; and $K_{X \sim X}(t)$ can be partitioned into all $\binom{S}{2}$ possible $K_{IJ}(t)$. As in the original version of Ripley's approach to point pattern analysis, these estimated partitioned K statistics would be transformed into the equivalent L statistics for easier interpretation. Figure 4.9a shows the artificial data for four species used to illustrate the multivariate pattern index $I(t)$ described in Section 4.1.5. Figure 4.10a analyses the same data and plots the estimates of $L_{X \sim X}(t)$ (upper), $L_{..}(t)$ (middle), and $L_{XX}(t)$ (lower). These results show

that while the arrangement of events is random, events of the same type are clustered, on average, and segregated from events of a different type. The next part of the figure illustrates the different scales and intensities of clumping of the individual species, with Type 2 having the smallest scale of strong clumping and Type 1 differing little from random (Figure 4.10b). Figure 4.10c summarizes the interspecific analyses for individual species, showing that species 3 and 4 have a high degree of negative association with events of other types over all scales. These could be further partitioned into particular species pairs, 1 and 2, 1 and 3, and so on. Although this analysis is more complicated than other approaches, it is also able to provide the most detailed information on the characteristics of the multispecies pattern.

There is another follow-up to the 'two at a time' comment of Lotwick & Silverman, and it is the observation that the relationship between any two species may be changed by the presence (or absence) of a third species. We have discussed this idea already in relation to the detection and evaluation of species associations as detected by presence and absence in sample units such as quadrats. In a spatially explicit context, we can consider using a Getis style map of Ripley's L -function scores based on univariate, bivariate, and trivariate analyses. We can imagine the situation where species A and B are negatively associated with each other (segregated) at small scales because of competition between them in areas of similar and preferred ecological conditions. At larger scales the two are found to be positively associated (aggregated) because the presence of large patches of a third species, C, excludes them both (examine the figures depicting the locations of trees of different species in the famous Lansing Woods example in Diggle's 1983 book, and elsewhere).

Condit *et al.* (2000) suggested analysing multispecies point pattern using a modification of Ripley's K , based on counts in circular bands or annuli of width Δt centred on individual events, rather than in circles. The statistic they suggested is:

$$\Omega_I(t) = [K_{II}(t + \Delta t) - K_{II}(t)] \div \{\lambda I[\pi(t + \Delta t)^2 - \pi t^2]\}. \quad (4.21)$$

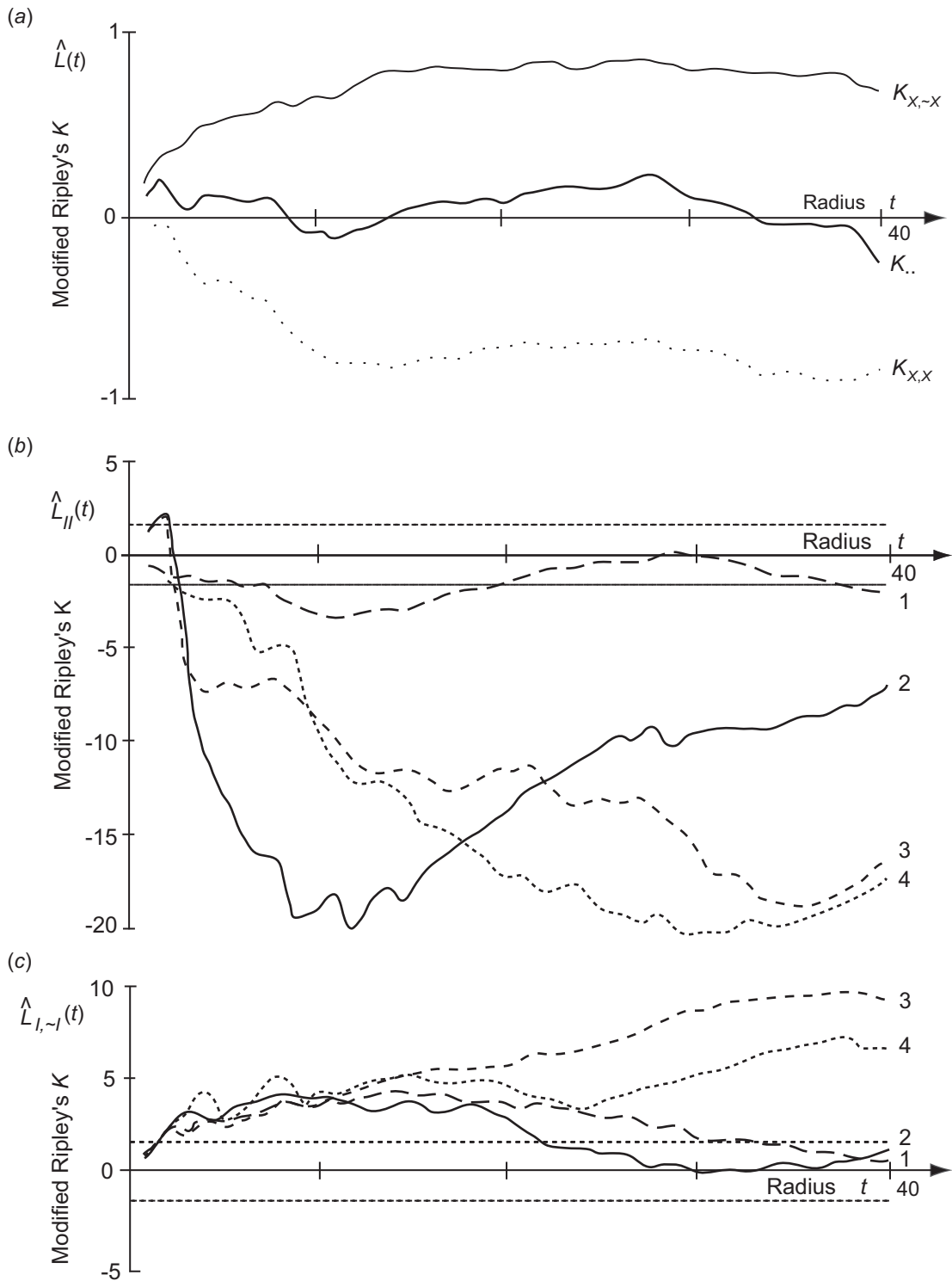


Figure 4.10 (a) Multivariate standardized Ripley's K analysis for all species: bottom line, conspecific pairs; middle line, all pairs; top line, interspecific pairs. (b) Standardized Ripley's K analysis for each species: conspecific pairs. (c) Multivariate standardized Ripley's K analysis for each species: all interspecific pairs.

While the divisor looks complicated, it is just the area of the circular band used to make the counts multiplied by the unit density of species I .

The use of rings rather than circles for event counts allows the isolation of specific distance classes, rather than including the short distances with the larger, as occurs with large-diameter circles. One disadvantage of this method is that the distance classes need to be broad, particularly for rare species, in order to avoid erratic-appearing curves due to zero counts. In addition, the choice of the width of the circular band used may be somewhat subjective. The difference between using circular bands rather than complete circles is that what is being studied is distance, rather than scale of pattern, as in the relationship between paired quadrat variance (PQV) and two-term local quadrat variance (TTLQV) described in Chapter 5.

Given the large range of methods available, a choice of method may seem difficult. Methods based on Ripley's K are popular, and for good reason: they are easy to use and to interpret and there is a range of such techniques that cover most kinds of point data. In general, they examine scale of pattern and they can deal with situations in which several scales of pattern are present. The hierarchy of neighbours approach (described in Chapter 3) does not use distance explicitly in the way that Ripley methods do and would provide a good complement to that set of methods. No single method can tell us everything we may want to know and so the use of two or three complementary methods is recommended, as usual.

4.2 Mark correlation function

The following methods are designed to investigate the interactions of neighbouring trees in a forest and appear in the works of Penttinen *et al.* (1992), Gavrikov & Stoyan (1995), and Stoyan & Penttinen (2000). This approach follows on from the bivariate methods described in Section 4.1.4, to take account of a quantitative characteristic (*mark*) associated with events, m_i ,

for example for the diameter of a tree; for more details, see Illian *et al.* (2008).

If μ is the mean value of m_i , then

$$\hat{K}_m(t) = \sum_{i=1}^n \sum_{j \neq i}^n w_{ij} I_t(i, j) m_i m_j, \quad (4.22)$$

and the observed value is compared with the expected value by calculating

$$\hat{L}_m(t) = t - \sqrt{\hat{K}_m(t)/\pi\mu^2}. \quad (4.23)$$

When \hat{L} is plotted as a function of t , large positive values indicate overdispersion of the marks and large negative values indicate their aggregation. Parallels with the interpretation of Ripley's K -function are obvious. The authors also pointed out that replacing $m_i m_j$ with $(m_i - m_j)^2$ in Eq. (4.22) produces what is essentially the equivalent of the sample, or experimental, variogram (see Chapter 6).

An artificial example (data in part (a)) is presented in Figure 4.11 in which the events are not clumped, but the values associated with them (diameter) are. Ripley's K -function analysis (Figure 4.11b) shows no evidence of clumping, but the mark correlation analysis does (Figure 4.11c). The authors suggested using a 'kernel' (smoothing) function as part of the calculation, but that may not be necessary since its only effect is to smooth the differences exhibited by different distances.

Goulard *et al.* (1995) provided an excellent example of the usefulness of this approach in a study of the clumps of sprouts of sweet chestnut, *Castanea sativa* Mill., in the Limousin region of France. In addition to the locations of coppiced clumps, four variables were measured: diameter, number of shoots before cutting, height at one year after cutting and height at three years after cutting. These were the 'marks' used in the analysis. The authors also measured soil depth to the granite beneath, at 120 locations, and produced an interpolated (Kriged) estimated surface (see Chapter 6) of soil depth for the whole study area. They found that the clumps were regularly dispersed, with diameter and number of shoots displaying negative autocorrelation at smaller distances. Heights were not strongly

correlated. The analysis showed that small clumps were aggregated in gaps between larger clumps and that heights could be related to their spatial correlation with local soil variables. This study provides a good example of the sophisticated and detailed analysis that the marked point process approach can offer, especially when used in combination with other forms of analysis.

Suzuki *et al.* (2008) used mark correlation analysis in a study of local size hierarchies and tree spacing in a forest of *Abies veitchii* and *Abies mariesii*. They found that this method was able to detect local size hierarchies that remained undetected by the more standard spatial autocorrelation measures. Finally, Ledo *et al.* (2011) have extended the method even further in describing an intertype mark correlation function that can be used to characterize relationships between different categories, such as among tree diameters for different tree species in a forest.

4.3 Ripley's K -function for inhomogeneous point pattern analysis

This section presents a modification of the familiar methods based on Ripley's K -function for the analysis of spatial point patterns, the arrangements of dimensionless point events in the plane, to cases in which the assumption that the underlying process is homogeneous and stationary is dispensed with. The point events may be all the same (univariate), of two different kinds (bivariate), or of several different species (multivariate). The same approach can also be adapted for mark correlation analysis when the point events have quantitative values associated with them. The major modification to the original method is in the calculation of the expected value of the counts in circles of a given radius, replacing the overall 'global' intensity of the point pattern with a 'regional' value, where the size of the region can be chosen either a priori by the user or determined based on one of several criteria using the data themselves. As a specific suggestion, we describe the use of a large circular region, radius T , centred on each

of the point events, for comparison with the usual statistic template of a smaller circle radius t , also centred on each point event. We provide a detailed description of the methods, examples of their application, and a guide to the interpretation of the results.

There is an extensive body of literature on the analysis of dimensionless events located in two or three dimensions, referred to as 'point pattern analysis' described in Section 4.1 (e.g. Diggle 1983; 2003). Almost all versions of this kind of analysis assume that the underlying process that gives rise to the pattern is both stationary (the same throughout the study region) and homogeneous, so that every location in the area under study has an equal probability of containing a point event. Most of these methods involve comparing the numbers of events observed in samples of a given size with the number expected on the null hypothesis of complete spatial randomness (CSR) and the overall intensity of the pattern (average number of point events per unit area of the study region). Where the pattern is known or suspected to be caused by an underlying process that is not stationary, in that it changes in intensity across the study area, or non-homogeneous, in that the positions of the events are not independent of each other, the comparison with CSR may not be very useful. Illian *et al.* (2008) discussed the possibility of dividing the inhomogeneous study area into subareas that meet the criterion of homogeneity. Shimatani & Kubota (2004) suggested a somewhat different approach in which, under the special condition of a gradient, the point process is modelled with a combination of a Neyman-Scott process and an inhomogeneous Poisson process. The method we describe here is less sophisticated, but more general. Under the conditions of non-stationarity or inhomogeneity, it makes some sense to derive the expected values for the observed counts in a Ripley-style analysis on the average number of points in a subarea rather than in the whole area of study. Ripley's K is based on counts in circles of a given radius centred on points in the pattern itself, and thus each observed count is associated with a particular location, the central point, and can be considered to be a 'local' score or statistic, in contrast to

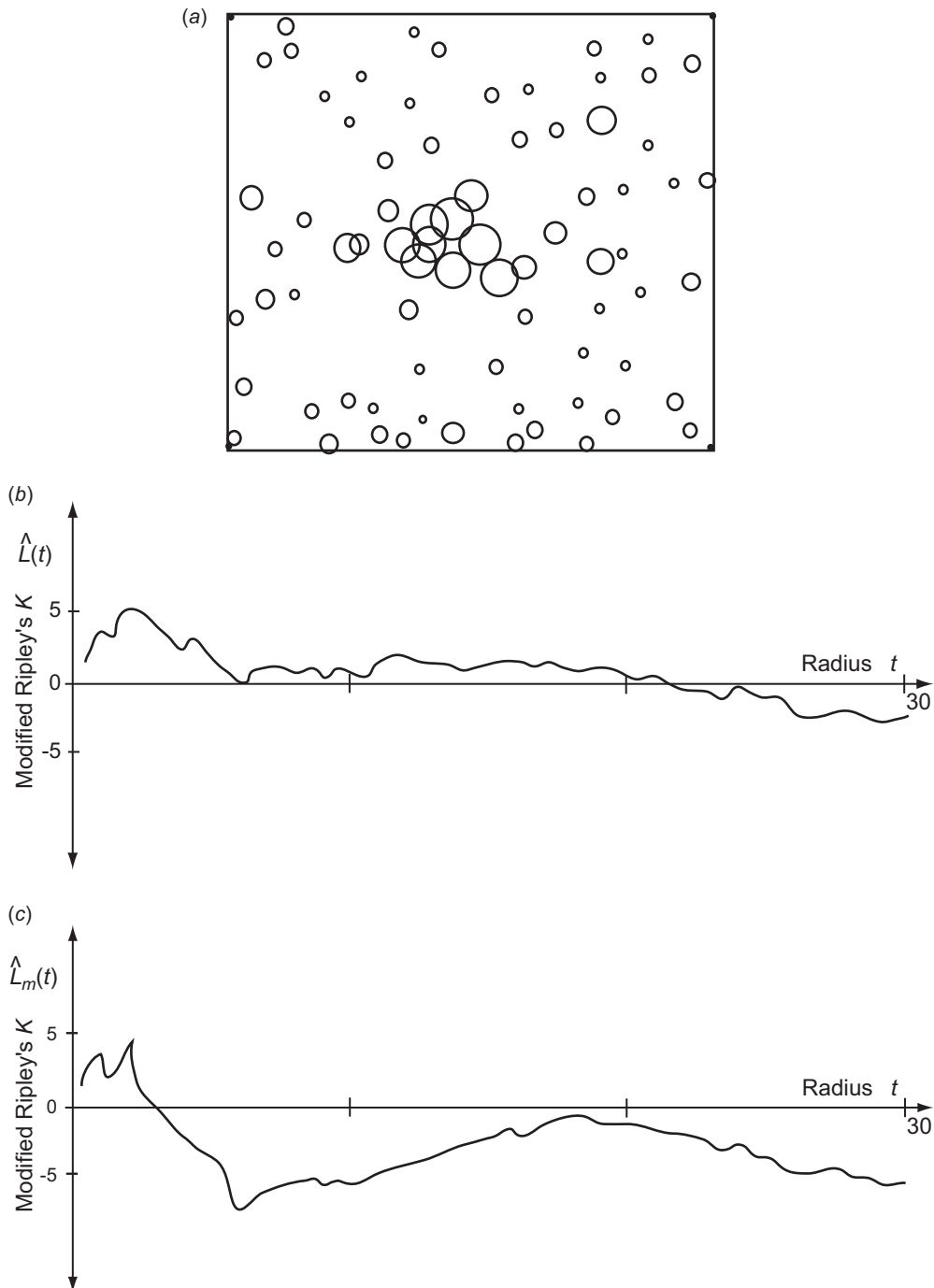


Figure 4.11 (a) Artificial univariate point pattern data with diameter characteristics (the dots indicate the size of the study area). (b) Standardized Ripley's K analysis on artificial univariate diameter data (positions only). (c) Mark correlation analysis on the same artificial univariate data, using diameter and position, where $\hat{L}_m(t)$ is the mark correlation statistic.

the overall intensity which is a 'global' value, and which can be used to produce a global statistic that compares the average local score with a global expected value. In the approach described here, the same local scores are compared with expected values localized to the same central point event and calculated from a regional, rather than global, intensity.

We can base the analysis of inhomogeneous patterns on methods that already exist, such as Ripley's K -function (Ripley 1976), which we have described in Section 4.1 above. This method is based on the concept that, if λ is the density of events per unit area, the expected number of events in a circle radius t centred on a randomly chosen point is $\lambda K(t)$, where $K(t)$ is a function that depends on the pattern of the events. For example, if the events are overdispersed, $K(t)$ will be close to 0 for short distances but increasingly positive for larger distances.

For any given distance, t , the statistic is based on counting all pairs of points separated by distances less than t . The statistic $\hat{K}(t)$ is an estimate of the function $K(t)$:

$$\hat{K}(t) = A \sum_i \sum_{j \neq i} w_{ij} I_t(i, j) / n^2. \quad (4.24)$$

Here, A is the area of the plot, $I_t(i, j)$ is an indicator function, taking the value 1 if the distance, d_{ij} , between points i and j is no greater than t , and 0 otherwise, and w_{ij} is a weight to correct for edge effects. The observed statistic $\hat{K}(t)$ is compared with this expected value by subtracting the observed from the expected (or vice versa) after a square root transformation (see Section 4.1.3).

In order to modify this approach to deal with inhomogeneous structure rather than CSR, a number of adjustments must be made.

Inherent in the original Ripley's K approach is a comparison between the observed pattern the null hypothesis of CSR. This is obviously useful for simple data analysis, but if we are interested in testing characteristics beyond just 'CSR versus non-CSR', a more sophisticated approach is needed to include null hypotheses that allow non-stationarity or non-homogeneity. To do so, we need to be able to compare

the observed and expected counts of point events in circles radius t centred on each of the point events, i . The difference is that the original formulation of Ripley's K takes the average of such counts and compares that average with its expected value; we need the same comparison for each individual count because the expected value will now depend on location, not just on circle radius and overall intensity. Let $c_i(t)$ be the observed count of events in a circle radius t centred on event i (exclusive of event i itself). Ripley's K was originally based on:

$$S_1 = \frac{1}{n} \sum_{i=1}^n c_i(t) - E \left[\frac{1}{n} \sum_{i=1}^n c_i(t) \right], \text{ but instead, we need to evaluate:}$$

$$S_2 = \frac{1}{n} \sum_{i=1}^n \{c_i(t) - E[c_i(t)]\}. \quad (4.25)$$

By making this substitution, and using the 'global' expectation based on stationarity and CSR, the two sums are the same and we get a statistic that is almost the same as the original K

$$\hat{C}(t) = \frac{A}{n} \left[\frac{1}{n} \sum_{i=1}^n \{c_i(t) - E_G(c_i(t))\} \right]. \quad (4.26)$$

Here the ' C ' refers to the circle-by-circle calculation, and the subscript ' G ' refers to the 'global' expected value based on the characteristics of the whole study area, with n point events and area A . The statistic, C , differs from K in that the expected value is subtracted, although we can easily consider $C'(t) = -C(t)$, and it differs from L in that the square root transformation has not been applied. The other difference between C and K as described here, is that in K , the edge correction appears in the weight included in the counting procedure, the 'observed', whereas in C , we have included the edge correction in the calculation of the expected value, leaving the observed as a simple count.

The global expected value can then be replaced by $E_R(c_i(t))$, based on the number of point events and the area of some subplot of the study's full extent (for

example, the density of point events in a circle of radius T centred on event i :

$$\hat{C}_R(t) = \frac{A}{n} \left[\frac{1}{n} \sum_{i=1}^n \{c_i(t) - E_R(c_i(t))\} \right] \quad (4.27)$$

or

$$\hat{C}_R(t) = \frac{A}{n} \left[\frac{1}{n} \sum_{i=1}^n \left\{ c_i(t) - c_i(T) \frac{a_i(t)}{a_i(T)} \right\} \right] \quad (4.28)$$

if the regional intensity estimate is based on a circle of radius $T > t$, centred on point event i , with the circle's area within the study area designated as $a_i(r)$, for any radius r .

In the original treatment of point pattern analysis, a square root transformation was applied to the difference between the observed count average and its expected value, in order to make the resulting statistic, called L , linear with radius, t . The same logic suggests that the most comparable and useful statistic for the analysis of non-stationary point pattern should include a square root transformation, giving:

$$\hat{L}_R(t) = \sqrt{\frac{A}{n}} \left[\frac{1}{n} \sum_{i=1}^n \left\{ \sqrt{c_i(t)} - \sqrt{E_R(c_i(t))} \right\} \right]. \quad (4.29)$$

The accompanying diagram, Figure 4.12, shows the result of analysis for a point pattern with a density trend in each of the x and y directions. The usual analysis detects a tendency to clumping at all scales, but the inhomogeneous approach shows that the pattern is approximately random, once the effects of the trend are removed.

This approach to the analysis of non-stationary point patterns can be extended to include the cases in which the point events have labels. First, the bivariate case with point events of two species, with each event having one of two labels indicating the category to which they belong, such as flowering versus non-flowering. The second case is multivariate where there are several different labels for the point events, such as the case of several species of trees in a mixed-wood

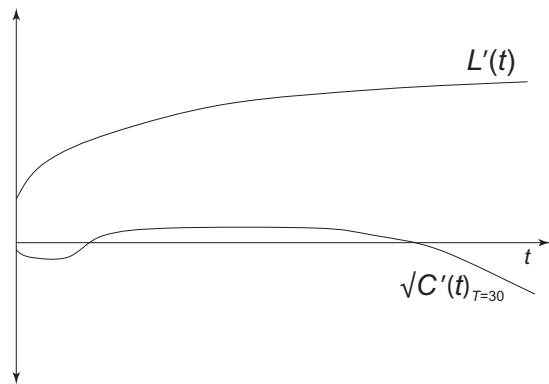


Figure 4.12 Showing the original modified Ripley's K statistic, $L'(t)$, and the new statistic for which the expected value is regional, not global, for a point process that has a trend in both the x and the y direction.

forest. The third case is that in which the events have quantitative rather than qualitative marks, such as tree height or diameter.

4.3.1 Bivariate and multivariate non-stationary point patterns

The non-stationarity point pattern statistic for the bivariate case is asymmetric, whereas for CSR and Ripley's bivariate $K_{1,2}$ the statistic is symmetric, with counts of events of Type 1 in circles centred on events of Type 2 and counts of events of Type 2 in circles centred on events of Type 1 estimating the same function. Because there are several types of non-stationarity possible, the statistic for the latter combination of events is:

$$\hat{C}_{R(1,2)}(t) = \frac{A}{n_2} \left[\frac{1}{n_1} \sum_{i=1}^{n_1} \{c_{i(1,2)}(t) - E_R(c_{i(1,2)}(t))\} \right]. \quad (4.30)$$

If the two categories are found to be aggregated, that may be attributable to the aggregation of the two kinds of plants within a random pattern of the plants of either kind, or it may result from the overall patchiness of all the plants considered together (cf. Dale & Powell

1994). The two possibilities can be distinguished by comparing the results of two different basic approaches to randomization.

- (1) Restricted randomization by re-labelling: the original locations of the events are retained, but their 'labels' are randomly re-arranged among the events. (This maintains the overall spatial structure of the pattern of locations.)
- (2) Complete randomization: reassignment of the positions and labels of the individual events, or equivalently, a Monte Carlo generation of the locations of the same numbers of the two species of point events as in the original data. A similar, but not identical approach is to use a Monte Carlo simulation of the data, with the expected number of events of each type determined by the original data, but with the actual number in a simulation being allowed to vary according to probabilistic rules.

By similar arguments, non-stationarity in the frequencies of the categories can be attributed to either non-stationarity in the set of locations of the events, or to non-stationarity in the frequency of the category to which each event belongs.

Here, there are several different categorical labels such as the species or age class for tree stems in a forest. The approach is closely based on the bivariate case, looking at pairs of species, of which there are $s(s-1)/2$ for all s species, or s different cases if we examine only non-conspecific pairs, of species A , for example, with all plants not of species A , ($I, \sim I$).

4.3.2 Quantitative marks: mark correlation

This case examines the situation when the point events have a quantitative attribute, such as age or height, as well as a location associated with each one, call the value m_i for event i . Following the model developed for the simple event counting approach described above, let $M_i(r)$ be the sum of all marks in a circle of radius r centred on event i , but excluding m_i

$$M_i(t) = \sum_{j=1}^n I_t(i, j) m_j - m_i = \sum_{j \neq i}^n I_t(i, j) m_j. \quad (4.31)$$

Then, the local-regional mark correlation statistic is:

$$\hat{C}_{R(m)} = \frac{A}{n} \left[\frac{m_i}{n} \sum_{i=1}^n \{M_i(t) - E_R(M_i(t))\} \right] \quad (4.32)$$

or

$$\hat{C}_{R(m)}(t) = \frac{A}{n} \left[\frac{m_i}{n} \sum_{i=1}^n \left\{ M_i(t) - \frac{a_i(t)}{a_i(T)} M_i(T) \right\} \right] \quad (4.33)$$

if the regional intensity is estimated from a circle radius T centred on event i .

This approach works well, but there are complications that we do not experience with standard point pattern analysis. The most obvious is the sensitivity of the analysis to the size of the region used to derive the 'expected value' for the count in any given circle. A series of analysis for each of a range of regional sizes may seem to run the risk of over-analysis, but such a series may provide more information than the choice of a single region size. In this description, we have concentrated on the use of a point-centred circle as the region for intensity estimation, there are a number of other possibilities, but this approach has the advantage of conceptual and computational simplicity (using the same calculations as for the local score) and it ties in with the use of circular templates for calculations, as in the nearest neighbour approach, Ripley's K as originally formulated, and the circumcircle approach described in Section 4.5, below.

For the cases where independence is not a reasonable null hypothesis, we must build in the constraints of trend in intensity or whatever form of non-stationarity is active in the process that produces the data. When developing restricted randomization procedures for testing our hypotheses, different forms of non-homogeneity must be considered. The treatment of non-homogeneous data and non-stationarity is an area of analysis with great potential for useful application in ecological studies.

Of course, non-stationarity is only one possible violation of the assumptions of the usual spatial analysis we have described. The possibility of anisotropic pattern must also be considered. Illian *et al.* (2008) included a discussion of the analysis of

point patterns' orientation, based either on the directions of nearest neighbours or on a subdivision of the circles used for counting events in a Ripley's analysis. The first is similar to elements of the fibre analysis we describe in Chapter 3 on lines and graphs: the graph edges between the nearest neighbour events (nodes) are the fibres that can be analysed for direction (see Figure 3.15). The second approach is described and illustrated in Dale (1999, pp. 227–231) in which the circle template of Ripley's K event counts is divided into directional sectors and the analysis proceeds as usual, but based on several direction sectors (hence several different plots of transformed counts against distance) which are kept separate to evaluate difference due to direction.

4.4 Point patterns in other dimensions

4.4.1 One dimension

The arrangement of events in one dimension can arise in many different ways in ecology: the positions of species boundaries along an environmental gradient, the heights of epiphytes up a tree trunk, encounters with individuals or nests along a line transect, and so on. Based on studies of boundaries on gradients, Dale

(1999) described several methods to study the arrangements of events in one dimension.

We can standardize the total length under study to the value 1, and then the n events, the x s, divide the interval 0 to 1 into $n + 1$ pieces of length u_i (see Figure 4.13a). Two statistics can then be used to help distinguish among different arrangements of the events:

$$W_n = \sum_{i=1}^{n+1} u_i^2 \quad (4.34)$$

and

$$h_n = \sum_{i=1}^n u_i u_{i+1}. \quad (4.35)$$

Tables of approximate critical values and guidance for the use of these two statistics are presented in Dale (1999). The statistic W_n detects the pairwise clumping of boundaries that produce unexpectedly short segments, because large values indicate a greater inequality of segment lengths. The statistic h_n measures the serial autocorrelation because large values indicate that short segments tend to be adjacent to other short segments and large segments tend to be adjacent to other large segments. A more detailed discussion of these statistics is provided in Dale (1999). For the purposes of this chapter, however, which has so far

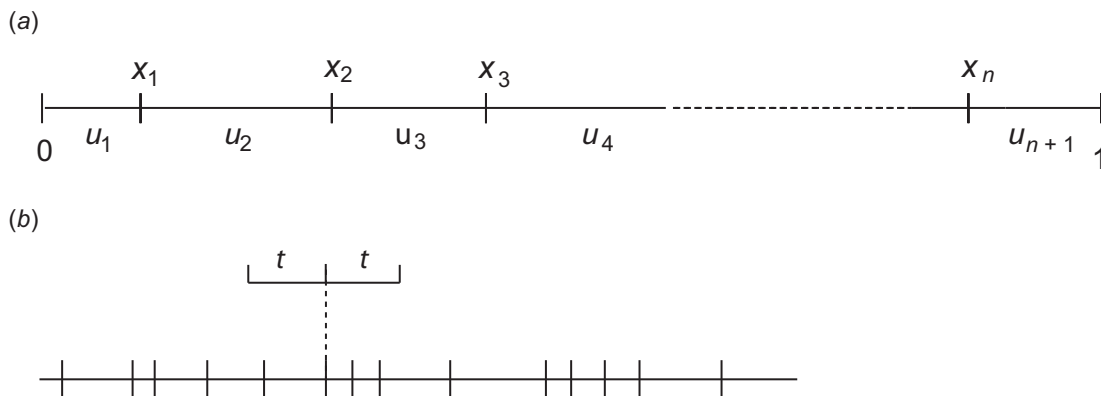


Figure 4.13 (a) Illustration of standardized one-dimensional transect data, with n events. (b) A line segment with n events, and the 't-bar' used for calculating the one-dimensional version of Ripley's K -function.

emphasized methods related to Ripley's K -function analysis, it is of interest to provide a one-dimensional version of that now-familiar technique.

A total sample line segment of length B in which n events occur is shown in Figure 4.13*b*. For a range of values, t , the number of events within distance t of each event is counted:

$$\hat{K}(t) = B \sum_{\substack{i=1 \\ i \neq j}}^n \sum_{\substack{j=1 \\ j \neq i}}^n w_i(t) I_t(i, j) / n^2, \quad (4.36)$$

where $w_i(t)$ is a weight that corrects for edge effects. If a bar of length $2t$ centred on event i is completely within the segment, $w_i(t) = 1$, otherwise it is the reciprocal of the proportion of that bar that is within the line segment (Figure 4.14*b*). Because the number of events expected to fall inside a bar of length $2t$ if the events occur randomly is $2nt/B$, we plot

$$\hat{L}(t) = t - \hat{K}(t)/2 \quad (4.37)$$

as a function of t . Values above zero indicate over-dispersion of the events and values below zero indicate clumping. An artificial example is given in Figure 4.14*a, b*, and a physical example of the sequence of rapids on the Winisk River in Northern Ontario (53° 30' N, 87° 20' W) is given in Figure 4.14*c, d*. In this map example, $W_m = 0.043$ and $h_m = 0.024$, neither of which are significant. A second physical example is presented in Figure 4.14*e, f*, from the Morris/Pipestone River, also in Northern Ontario (52° 15' N, 90° 45' W); here $W_m = 0.089$ and $h_m = 0.027$. The first is significant, indicating that the rapids are clumped, but the second is not, indicating that there is no tendency to have clusters of short inter-rapid sections of the river.

A simple and obvious modification of Eq. (4.36) produces a bivariate version of Ripley's K in one dimension. As an extension to calculations in one dimension, Okabe & Yamada (2001) explained the univariate and bivariate forms of Ripley's K -function analysis when the events occur in a two-dimensional space, but are constrained to a network of one-dimensional structures. The example they gave is of fast-food stands on a network of streets, or fast-food

stands and subway stations for the bivariate case. Applications to ecological studies such as the occurrence of species of aquatic invertebrates in the water channels of a delta, or flowering and non-flowering shoots on a system of rhizomes are obvious. In the ecological literature, there is at least one example of this approach, already mentioned in Chapter 3: Spooner *et al.* (2004) have analysed the spatial arrangement of *Acacia* trees on a road network in Australia. That study provides a useful model for future studies of the spatial relationships of organisms on anthropogenic linear structures. This approach ties in very closely to the analysis of linear structures and of point events and linear events described in Chapter 3.

4.4.2 Lacunarity

The term 'lacunarity' is derived from the Latin '*lacuna*', meaning a literal or metaphorical hole, and so the concept of lacunarity refers to the characteristics of the holes or gaps in a spatial structure. Several different methods for calculating a measure of lacunarity have been proposed, but Plotnick *et al.* (1996) recommend the 'gliding box' (a 'moving window' template) method of Allain & Cloitre (1991). Picture a string of events in one dimension with possibly irregular spacing; a box of length r is placed at the beginning of the set and the number of events that lie within it are counted. The box is moved one unit along the series and the number counted again, and so on, as illustrated in Figure 4.15. The first and second moments for the frequency distribution of the number of events per box are then determined for boxes of size r , call them $m_1(r)$ and $m_2(r)$. The measure of lacunarity for box size r is

$$\Lambda(r) = m_2(r)/[m_1(r)]^2. \quad (4.38)$$

The graph of lacunarity as a function of box size is usually presented in a double-log form: $\log[\Lambda(r)]$ as a function of $\log(r)$, as in Figure 4.16.

Plotnick *et al.* (1996) provided guidelines for the interpretation of the lacunarity index as a function of box size. Random data produce a curve that is concave

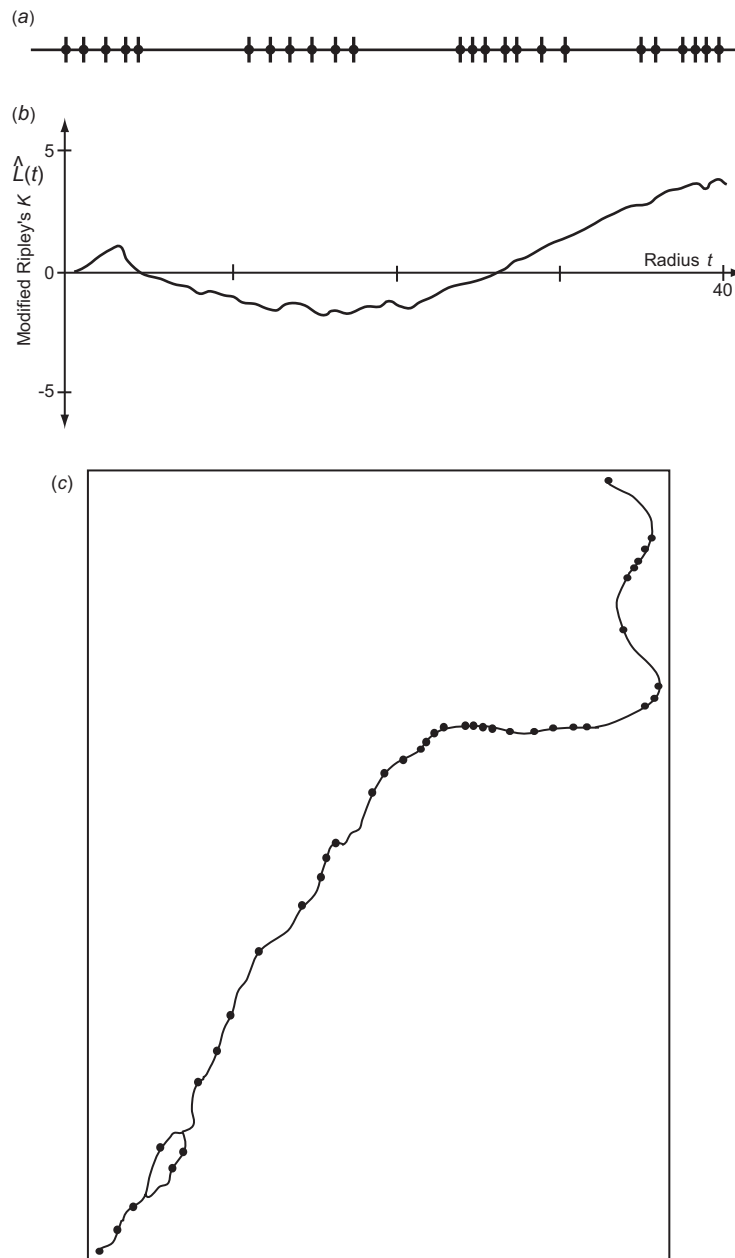


Figure 4.14 (a) Artificial one-dimensional transect data (clumps). (b) Standardized Ripley's K analysis on one-dimensional transect data. There is overdispersion at both very small and very large scales. (c) Rapids on the Winisk River. (d) Standardized Ripley's K analysis of the Winisk River rapids data. (e) Rapids on the Morris/Pipestone River. (f) Standardized Ripley's K analysis of the Morris/Pipestone River rapids data.

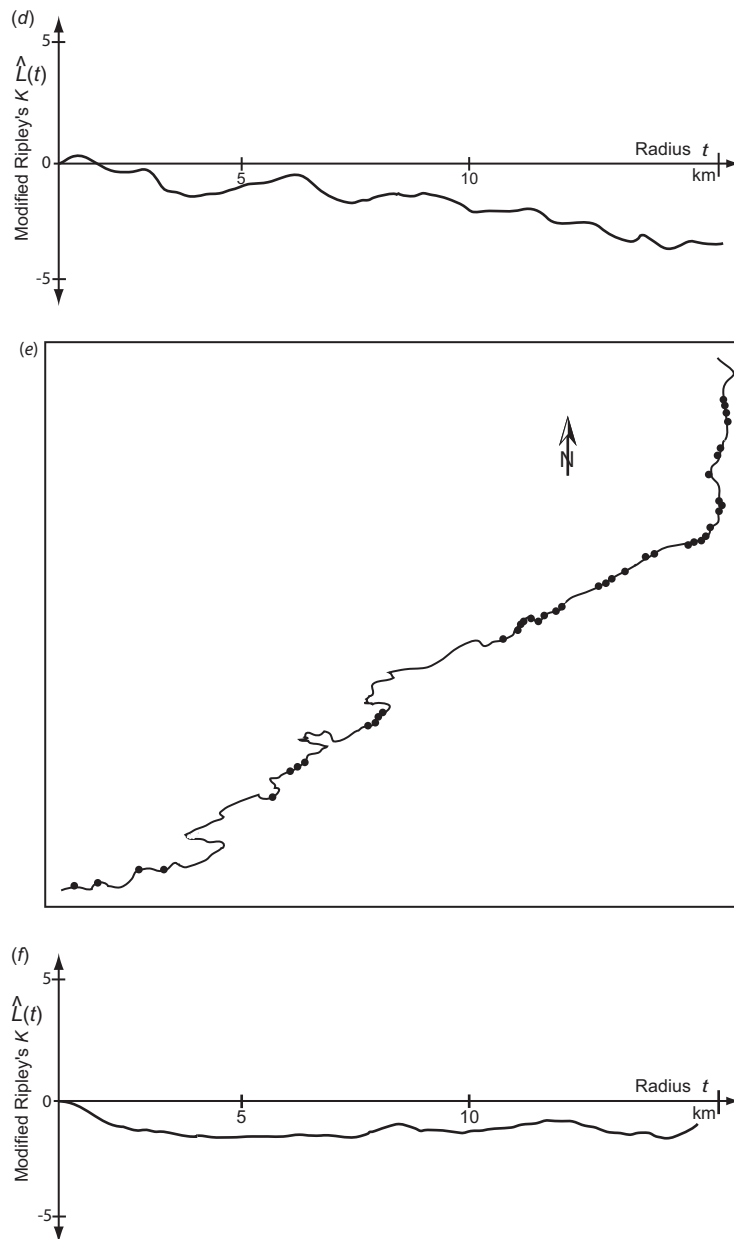


Figure 4.14 (*cont.*)

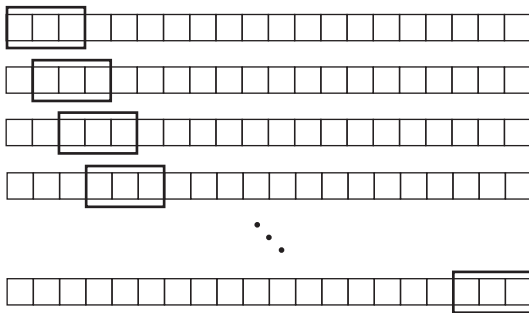


Figure 4.15 In lacunarity analysis, a ‘gliding box’ moves along a string of events in one dimension (redrawn from Dale *et al.* 2002).

upward; clumped data of the same density produce curves that have greater lacunarity and that are initially concave downward; and regularly spaced data of the same density produce curves that are initially straight and have lower lacunarity. The shape of the double-log curve depends only on aggregation and is independent of the overall density; density determines the curve’s maximum. Plotnick *et al.* (1996) suggested that for data consisting of randomly placed clumps, the log-log lacunarity curve declines gradually with increasing box size to a break point corresponding to the size of the clumps. Beyond this break point, the plot declines more rapidly and is concave upward. They suggested that lacunarity curves of one-dimensional sets have distinct breaks in slope corresponding to distinct scales within the sets. Our own investigations (Dale 2000) suggested that the method is not that precise in determining the scale or patch size in these kinds of patterns, but the method is still popular, particularly in its two-dimensional form, and lacunarity remains part of the conceptual frameworks of spatial analysis (Dong 2009).

4.4.3 Three dimensions

The analysis of patterns in three dimensions has received less attention than two-dimensional analysis, in part because such data may be encountered less often. Many of the methods described for two dimensions can

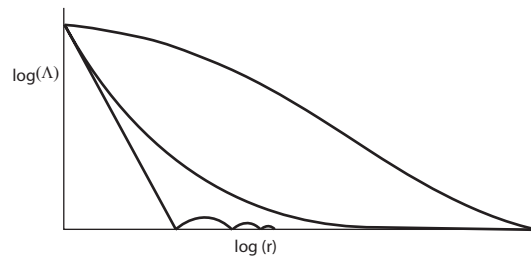


Figure 4.16 A graph of lacunarity as a function of box size. Top: clumped events; middle: random data; bottom: regularly spaced events.

be adapted for use in three, for example, the comparison of event–event nearest neighbour distance distribution with the distribution of random point–event distances can probably be transferred directly. König *et al.* (1991) described the adaptation of many of the methods described above for two dimensions for use with three-dimensional data. Muggleston (1996) described an approach that uses the Dirichlet tessellation for analysing such data. The tessellation is used as the basis for a randomization test of the arrangement of labels for bivariate data. In both these studies the subject of discussion was cellular: the position of cells in tissue or of the centromeres of chromosomes within cells.

We can also modify Ripley’s K -function analysis for three dimensions, as described by Baddeley *et al.* (1987) and König *et al.* (1991) among others (e.g. Mamaghani *et al.* 2010). With the usual notation, and V being volume, calculate:

$$\hat{K}(t) = V \sum_{\substack{i=1 \\ i \neq j}}^n \sum_{\substack{j=1 \\ j \neq i}}^n w_i(t) I_t(i, j) / n^2. \quad (4.39)$$

That is, count the number of events centred on an event within a sphere of radius t of each event. The edge correction factor $w_i(t)$ is 1 if the sphere, centred on i and radius t , is completely within the study volume; otherwise, it is the reciprocal of the proportion of the sphere that lies within the study volume. Because the volume of the sphere is $4\pi t^3/3$, calculate:

$$\hat{L}(t) = t - \sqrt[3]{3 \hat{K}(t) / 4\pi}. \quad (4.40)$$

Under CSR, the expected value is 0 and significant departures from 0 are interpreted in the usual way. Extensions of this approach to bivariate and multivariate analysis will proceed with simple modifications as described for two-dimensional data.

In addition to the adaption of Ripley's K , König *et al.* (1991) described three-dimensional versions of the 'event-to-nearest-event' and 'random-point-to-nearest event' statistics, the G -function and F -function described in Section 4.1.2. They also introduced a three-dimensional marked point process analysis such as we discussed for two dimensions in Section 4.2 above. These three-dimensional approaches have, so far as we know, been applied mainly in the context of the positions of cells in tissue, and rarely to ecological examples. The best example we have found is by Everhart *et al.* (2011) who used an extension of nearest neighbour analysis to examine the spatial aggregation of brown rot in the canopies of sour cherry trees which were mapped intensively. Once it becomes well-known that methods for three-dimensional pattern analysis are available and easy to apply, we expect to see applications of these methods in ecological studies. As only one example, characterizing the three-dimensional positions of leaves in a layered forest canopy would be an important first step toward evaluating and modelling the infiltration of light to lower strata of the forest.

4.5 Circumcircle methods

The next set of methods we describe are conceptually related to several of the approaches already described, including Ripley's K -function and neighbour networks (also see wavelets, Chapter 5). Expanding on the idea of counting events in circles for completely mapped point data, we can consider ways of locating the circles, other than centering them on single events in the pattern, as in Ripley's K . Each trio of events in a mapped pattern defines a triangle and each triangle has associated with it a circle that goes through all three events, the circumcircle (Dale & Powell 2001). The close relationship with Ripley's approach is based on counting events in circles. There is also a

relationship, based on the use of the circumcircle with the definition of one of the neighbour networks described above, the Delaunay triangulation, because empty circumcircles define that network. The basic method can also be seen as an extension of Ripley's K , called a second-order method because it looks at pairs of events, to a higher-order statistic, comparable to the third-order point process measure described by Schladitz & Baddeley (2000). Both the third-order statistic and the circumcircle approach can be seen as closely associated with the Delaunay triangulation as one of the common reference spatial graphs described in Chapter 3.

4.5.1 Univariate analysis

For a total area of mapped plot, A , and n events in it, the average density is $\lambda = n/A$. There are approximately $n^3/6$ triplets of events and therefore the same number of circumcircles. For the k th circumcircle, let n_k be the number of events inside it (excluding the three that define its triangle) and let a_k be the area of the circle that is within the sample plot. The expected number of events in the circle is $e_k = (n-3) a_k / A$, based on the usual hypothesis of CSR. The Freeman-Tukey standardized residual can be used to compare the observed and expected numbers of events:

$$z_k = \sqrt{n_k} + \sqrt{n_k + 1} - \sqrt{4e_k + 1}. \quad (4.41)$$

Values of z less than -1.96 can be considered to indicate gaps and values greater than 1.96 indicate patches, but any region of low density may have many overlapping 'gap' circles and any region of high density may have many overlapping 'patch' circles.

To distinguish among the overlapping patch or gap circles indicated by high or low values of z , we can define the 'best' patch and gap circles as those that have the greatest contrast with their immediate surroundings. To find these, count the number of events in a ring around circle k that has an area equal to the circle; if the radius of the circle is r_k , then the ring has width $(\sqrt{2} - 1) r_k$. If the number of events in the ring is p_k with expected value f_k , then the standardized residual for the outer ring is:

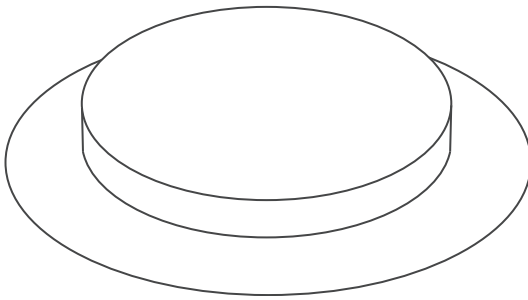


Figure 4.17 The 'boater' wavelet used in circumcircle analysis.

$$\varsigma_k = \sqrt{p_k} + \sqrt{p_k + 1} - \sqrt{4f_k + 1}. \quad (4.42)$$

The circle's residual, z_k , can then be combined with the ring's residual, ς_k , to produce a measure of the contrast between the densities of the circle and the ring:

$$Z_k = (z_k - \varsigma_k) / \sqrt{2}. \quad (4.43)$$

Z is calculated using a double circle template, which can be considered to be a wavelet, closely related to the 'French top hat', but in one more dimension, which we have termed the 'boater' wavelet (Figure 4.17; Dale & Powell 2001). Section 5.6 in the following chapter gives more detail on wavelets and their use in spatial analysis, but the general approach is to evaluate the similarity in structure of a localized template (the wavelet) with the data. As in those other forms of wavelet analysis, the value of Z measures how well the data match the shape of the template, here the double circle. The average Z^2 can be plotted as a function of the circle radius and peaks in this graph will reflect the sizes of patches and gaps in the pattern. To distinguish between the two, we can plot Z^2 as a function of the radius for positive residuals only, Z_P^2 , thus showing patch sizes, and then separately for negative residuals, Z_N^2 , thus showing gap sizes. Dale & Powell (2001) gave an example of this technique.

For some applications, it is desirable for the results of the analysis to be spatially explicit. Here, the z or Z score of each circle in a particular size class could be associated with the centre of the circle. In that way, a contour map of the scores could be produced for each

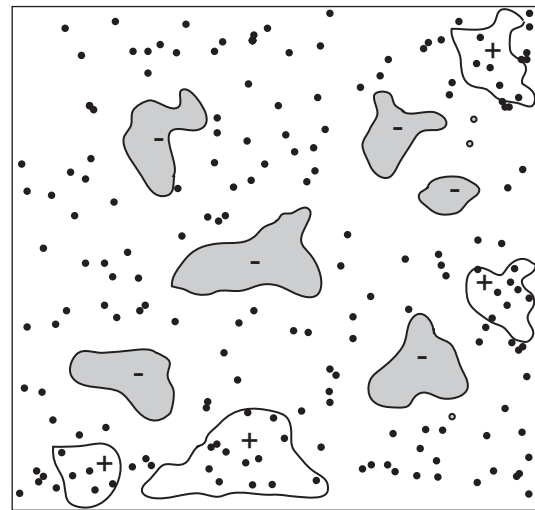


Figure 4.18 Contour map of significant patches ('+') and gaps ('-') based on Z scores of artificial univariate data.

of several size classes or scales. An illustration of the circumcircle technique is provided in Figure 4.18 where the shaded polygons indicate clusters of the centres of significant gap circles and empty polygons indicate clusters of the centres of significant patch circles. One feature of the relationship between a triangle and its circumcircle is that the centre of the circle may lie well outside the triangle, and the circle's area may be much bigger than the triangle's. This feature may affect our interpretation of the results.

4.5.2 Bivariate analysis

The bivariate version of this approach is a straightforward adaptation of the univariate version: Type 1 and Type 2 events are counted in circles based on triplets of Type 1 events, and in circles based on triplets of Type 2 events. The four different counts are kept distinct; this procedure makes the analysis truly asymmetric, unlike the Ripley's K -function approach. For example, when used with the positions of canopy trees and seedlings, we can determine whether seedlings tend to be found in canopy gaps and thus whether their occurrence is affected by gap size. We can also use this approach to

determine whether there are tree gaps that have significantly few seedlings in them. This method provides somewhat different information than the symmetric bivariate K -function, which detects the scales at which the two types of events are aggregated and the scales at which they are segregated.

Specifically, let n_i be the number of Type 1 events in a circumcircle based on Type 1 events, with area a_i , giving a standardized residual of z_i . Let m_i be the number of Type 2 events in the same circle and let y_i be the associated standardized residual. To examine the response of Type 2 events to Type 1 gaps, we can plot the mean and variance of y_i as a function of a_i for circles with $n_i = 0$, or plot the same values for circles with $z_i < -1.96$. This asymmetric approach to the analysis reflects the asymmetry of the biological processes; the positions of the canopy trees are expected to influence the presence of seedlings, but not the other way around. For different ecological situations, for example in studying the spatial relationships of two different species of canopy tree or alpine meadow forb, the counts in both kinds of circle (based on Type 1 and based on Type 2) could be used in the analysis.

A second approach to evaluating the relationship between the two kinds of events is to calculate covariance as a function of scale (circle area), using either the circumcircle or the double circle template, the boater wavelet described in Section 4.5.1. For the latter, if there were no edge effects, the covariance could be based on the squares of the differences between the observed counts of events in the inner and outer circles, such as $(n_i - p_i)^2$, $(m_i - q_i)^2$ and $(n_i + m_i - p_i - q_i)^2$. Because the circles can intersect the edge, we need to adjust for the area within the study area, again using standardized residuals.

In the univariate case, the circle and ring counts, n_i and p_i , were converted to standardized residuals, z_i and ζ_i . In the same way, the counts of a second type of event can be converted to standardized residuals, y_i and η_i and the total counts of both kinds to w_i and ξ_i . For an individual circumcircle, a covariance score can be calculated, using only the circle itself, as:

$$c_i = (2w_i^2 - y_i^2 - z_i^2)/2. \quad (4.44)$$

Using the boater wavelet, in the univariate case, the standardized residuals, z_i and ζ_i , are combined to form a residual of their difference, Z_i . For the bivariate situation, the other residuals are also combined to form difference residuals:

$$Y_i = (y_i - \eta_i)/\sqrt{2} \quad \text{and} \quad (4.45)$$

$$W_i = (w_i - \xi_i), \quad (4.46)$$

and an overall covariance score is

$$C_i = (W_i^2 - Y_i^2 - Z_i^2)/2. \quad (4.47)$$

For a particular range of radius values, R , the variances are then

$$\begin{aligned} V_Z(R) &= \text{average of } Z_i^2 \text{ for all } i \text{ with } r_i \text{ in } R, \\ V_Y(R) &= \text{average of } Y_i^2 \text{ for all } i \text{ with } r_i \text{ in } R, \\ V_W(R) &= \text{average of } W_i^2 \text{ for all } i \text{ with } r_i \text{ in } R. \end{aligned} \quad (4.48)$$

The covariance for the range R is then

$$C(R) = (V_W(R) - V_Z(R) - V_Y(R))/2. \quad (4.49)$$

The covariance is plotted as a function of R and positive and negative peaks in that plot are interpreted as the scales of aggregation and segregation of the two kinds of event (cf. Dale & Powell 1994).

For some applications, it is desirable to make the results of point pattern analysis spatially explicit. As described above, Getis & Franklin (1987) made contour maps of the K -function values of the events and interpolated points, for each of several radii. Extending that approach, the z or y score of each circle in a particular size class could be associated with the centre of the circle. In that way, a map of the scores can be produced for each of several radius ranges or scales. More simply, we can plot the centres of circles of a particular radius class, using two different symbols, one for values less than -1.96 and one for values greater than 1.96 . These maps, 'circle score maps', show the positions and extent of the centres of significant patches and gaps. Using the combined residuals, such as Z , Y or C , rather than just the inner circle residuals, z , y or c , reduces the number of scores to be plotted and should make them more informative.

4.5.3 Multivariate analysis

As with other univariate and bivariate analyses described in this chapter, the extension of circumcircle analysis to multivariate data is both straightforward in application and complex in the interpretation. For the analysis using Ripley's K , we recommended partitioning the total counts into 'con-specific' and 'interspecific', and then into the components ' I,I ', ' $I,\sim I$ ' and ' I,J '; the same recommendation applies to the circumcircle approach to multivariate spatial analysis.

Two examples of the multivariate circumcircle analysis are shown in Figure 4.19. The data are from one quadrant of the Lansing Woods data set (cf. Gerard 1969; Diggle 1983). For Maples we give the range and average value of z as a function of circumcircle area for the I,I ; and $I,\sim I$ combinations. The results consistently show larger numbers of congeners in smaller circles and fewer stems of different genera in the smaller circles. This approach provides some insights that complement the results from different kinds of analysis.

An additional and interesting analysis would be to calculate species diversity and species evenness for each circle, now including the three events that define it. The i th circle has $n_i + 3$ events and let p_j be the proportion of the events that belong to species j . A measure of diversity, D , can be calculated as Simpson's index (see Chapter 10) also with a measure of evenness, or equality of representation, derived from it. A spatially explicit result could then be the set of non-overlapping circumcircles (or elements of any other locational template) with diversity scores above a given threshold superimposed on the original map of events. There will be more discussion of diversity and of local measures of diversity for spatial analysis in Chapter 10 of this book.

4.6 Concluding remarks

Although, in this chapter, a wide range of data types and approaches to analysis have been discussed, the coverage is not exhaustive (Table 4.2). It is very

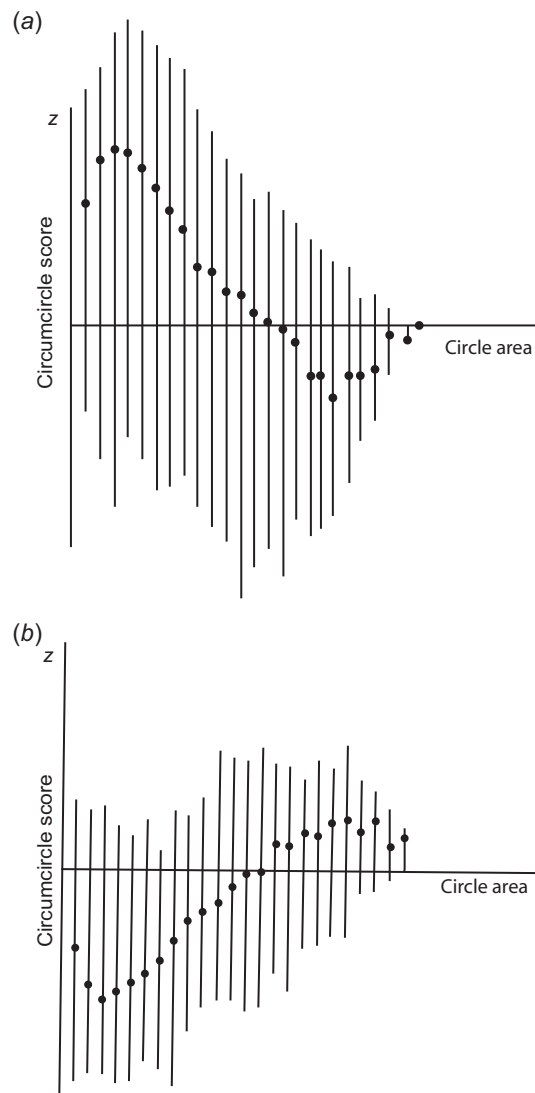


Figure 4.19 Multivariate circumcircle analysis. (a) The z scores, mean and range, as a function of circle size, for Maples: congeneric analysis. (b) The z scores, mean and range, as a function of circle size, for Maples: intergeneric analysis.

possible that the practising ecologist will encounter situations in which different kinds of data are met or different techniques of analysis are needed. These situations may be completely novel, in which case ingenuity and advice from analytical specialists may

Table 4.2 Summary of the spatial analysis methods presented in Chapter 4

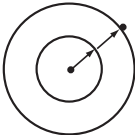

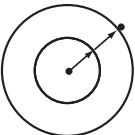

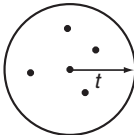
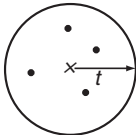
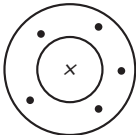
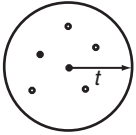
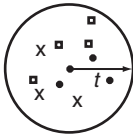


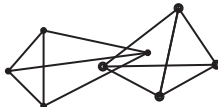


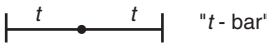
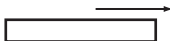
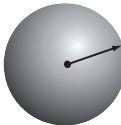

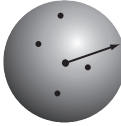
Spatial analysis method	Template	
Points		
Nearest neighbour		
	Expanding circle based on event	Simple linkage
Refined nearest neighbour		
	Expanding circle based on event or random point	Simple linkage
Univariate K		
	Expanding circle based on event	
Getis		
	Expanding circle based on event or random point	
Condit		
	Rings centred on events	
Bivariate K		
	Expanding circle	

Table 4.2 (cont.)

Spatial analysis method	Template	
Points		
Multivariate K	 Expanding circle	
Dixon	 Simple link	 Network of neighbours
Reich <i>et al.</i>	 Links to own type	
Mark correlation	 Expanding circle	
Events networks	 Links	
One-dimensional Ripley's K	 "t - bar"	
One-dimensional lacunarity	 Moving window/gliding box	
Three-dimensional nearest neighbour	 Expanding sphere	 Simple link
Three-dimensional Ripley's K	 Expanding sphere	

be required, or they may have been encountered before, but are not easy to find in the literature. We will describe one such situation for the purposes of illustration.

Many of the methods used for the analysis of the positions of events in two dimensions are based on the assumption that the events can be adequately represented as dimensionless points in a plane. In the analysis of a particular set of data, it may become clear that that assumption is not sufficiently realistic and the events should be treated as circles of non-zero radius: what then? This is one situation that has been encountered before, and the researcher can follow the treatment by Simberloff (1979), who studied the nearest neighbour assessment of the patterns of events that are circles, not points. The approach is illustrated using data such as the positions of ant-lion pits and ant nests. There is even a discussion of solving the same problem in

three dimensions, considering the dispersion of spheres, instead of circles.

In developing recommendations on which methods to use, it will have become clear to the reader of this chapter that the set of methods based on the concept of Ripley's *K*-function covers many different kinds of data and a range of situations. That set of methods has much to recommend it, although there is ongoing debate about the relative advantages of using whole circles as the template for counts (in Ripley's original method) or a 'de-cumulated' version based on rings of different widths. There may be a usefulness in linking these methods to the explicit development of their related spatial graphs (nearest neighbour, distance threshold, Delaunay triangulation, etc.) yet to be exploited. The decision on the method to use will depend, of course, on the data and the question being asked, but we suggest using two or more complementary approaches, so as not to miss important features of the data.